LBL-12556

Lawrence Berkeley Laboratory
UNIVERSITY OF CALIFORNIA

Materials & Molecular
Research Division

THE SYNTHESES AND ELECTRONIC STRUCTURES OF DECAMETHYLMETALLOCENES

John Lawrence Robbins
(Ph.D. thesis)

April 1981

Prepared for the U.S. Department of Energy under Contract W-7405-ENG-48

a

THE SYNTHESES AND ELECTRONIC STRUCTURES OF DECAMETHYLMETALLOCENES

John Lawrence Robbins

ABSTRACT

The synthesis of decamethylmanganocene ($(\eta\text{-}C_5(CH_3)_5)_2Mn$ or $(Me_5Cp)_2Mn$) is described. Magnetic susceptibility and electron paramagnetic resonance (EPR) studies show that $(Me_5Cp)_2Mn$ is a low-spin, 17-electron compound with an orbitally degenerate, $^2E_{2g}$ $[e_{2g}^3 a_{1g}^2]$ ground state. This is to be contrasted with Cp_2Mn, which possesses a high-spin, $^6A_{1g}$ $[e_{2g}^2 a_{1g}^1 e_{1g}^2]$ electronic configuration. An X-ray crystallographic study of $(Me_5Cp)_2Mn$ shows that it is a monomeric, D_{5d} decamethylmetallocene with metal to ring carbon distances that are about 0.3 Å shorter than those determined for high-spin manganocenes. Decamethylmanganocene is rather inert with respect to ring loss and hydrolysis, but it does undergo reversible one-electron oxidation and reduction reactions to yield isolable, low-spin 16- and 18-electron derivatives, $[(Me_5Cp)_2Mn]PF_6$ and $Na[(Me_5Cp)_2Mn]$. These two compounds are unique in that reduced or oxidized forms of high-spin manganocenes are unknown. The results indicate that complete alkylation of the cyclopentadienyl ring significantly enhances its ligand field strength. Studies of other first transition series decamethylmetallocenes support this conclusion.

The syntheses of new $(Me_5Cp)_2M$ (M = Mg,V,Cr,Co, and Ni) and $[(Me_5Cp)_2M]PF_6$ (M = Cr,Co, and Ni) compounds are described. In addition, a preparative route to a novel, dicationic decamethylmetallocene, $[(Me_5Cp)_2Ni](PF_6)_2$ is reported. Infrared, nuclear magnetic resonance, magnetic susceptibility, and/or X-ray crystallographic studies indicate that all the above compounds are D_{5d} or D_{5h} decamethylmetallocenes with low-spin electronic configurations. The decamethylvanadocene cation is apparently coordinatively unsaturated. A paramagnetic acetonitrile complex ($[(Me_5Cp)_2V(NCCH_3)]PF_6$) and a diamagnetic, dicarbonyl derivative ($[(Me_5Cp)_2V(CO)_2]PF_6$) of the cation can be prepared, but the isolation of pure $[(Me_5Cp)_2V]PF_6$ has thus far proven elusive.

Cyclic voltammetry studies verify the reversibility and the one-electron nature of the $(Me_5Cp)_2M \rightleftarrows [(Me_5Cp)_2M]^+$ (M = Cr,Mn,Fe, Co,Ni), $[(Me_5Cp)_2Mn]^- \rightleftarrows (Me_5Cp)_2Mn$ and $[(Me_5Cp)_2Ni]^+ \rightleftarrows [(Me_5Cp)_2Ni]^{2+}$ redox reactions. These studies reveal that the neutral decamethylmetallocenes are much more easily oxidized than their metallocene counterparts. This result attests to the electron-donating properties of the ten substituent methyl groups.

Proton and carbon-13 NMR data are reported for the diamagnetic Mg(II), Mn(I), Fe(II), Co(III), and Ni(IV) decamethylmetallocenes and for $[(Me_5Cp)_2V(CO)_2]^+$. Magnetic susceptibility and EPR studies indicate the following ground state assignments for the paramagnetic decamethylmetallocenes: $^4A_{2g}[e_{2g}^2\ a_{1g}^1]$ for the 15-electron compounds $(Me_5Cp)_2V$ and $[(Me_5Cp)_2Cr]^+$; $^3E_{2g}[e_{2g}^3\ a_{1g}^1]$ for the 16-electron compounds $(Me_5Cp)_2Cr$ and $[(Me_5Cp)_2Mn]^+$; $^2E_{2g}[e_{2g}^3\ a_{1g}^2]$ for the 17-electron compounds $(Me_5Cp)_2Mn$

and $[(Me_5Cp)_2Fe]^+$; $^2E_{1g}[e_{2g}^4\ a_{1g}^2\ e_{1g}^1]$ for the 19-electron compounds $(Me_5Cp)_2Co$ and $[(Me_5Cp)_2Ni]^+$; $^3A_{2g}[e_{2g}^4\ a_{1g}^2\ e_{1g}^2]$ for the 20-electron compound, $(Me_5Cp)_2Ni$.

The UV-visible absorption spectra of the 15-, 18- and 20-electron decamethylmetallocenes are also reported. Assignment schemes are proposed for the absorptions due to d-d transitions. A ligand field analysis is used to derive the ligand field splitting parameters Δ_1 and Δ_2 and the Racah electron repulsion parameter, B. A comparison of these parameters with those previously reported for the isoelectronic Cp_2M compounds reveals that the net ligand field splitting is larger in the permethylated compounds than in the unsubstituted derivatives. The parameter B is also larger in the peralkylated derivatives, indicating increased electron density at the metal center.

Table of Contents

Acknowledgements

I would like to first thank those who contributed their time, skills and enthusiasm at various stages of this work. Professor James Smart provided the initial impetus for this project and was more than generous in allowing me the time to pursue my own scientific interests during its progress. I am indebted to Dr. Norman Edelstein, Professor Richard Andersen, and Professor Ken Raymond for their friendship, support and valuable suggestions. For their help in performing various measurements, thanks go to Dr. Norman Edelstein and Professor Brock Spencer (EPR spectroscopy) and Professor Stephen Cooper (electrochemistry). The X-ray crystallographic studies are due to the diligent efforts of Dr. Derek Freyberg and Dr. Fred Hollander of Ken Raymond's research group.

Finally, thanks go to those who made my stay in Berkeley such a memorable one. My labmates Buzz Curtis, Barry Pinsky, and Al Sievert were the best one could ask for. Their cooperation, support, and humor were geniunely unique. Special thanks to Buzz for being a close friend both in and out of the lab. Thanks go to Jim Barrett, Jim Lindstrom, John Bolt, and Jon Newman for putting up with my eccentricities and being there when I needed a friend.

This work was supported by the Director, Office of Energy Research, Office of Basic Energy Sciences, Chemical Sciences Division of the U.S. Department of Energy under Contract No. W-7405-ENG-48.

List of Tables

List of Figures

List of Figures

LBL- 12556

THE SYNTHESES AND ELECTRONIC STRUCTURES OF DECAMETHYLMETALLOCENES

John Lawrence Robbins

Ph.D. Thesis

Materials and Molecular Research Division
Lawrence Berkeley Laboratory
and
Department of Chemistry
University of California
Berkeley, California 94720

This work was supported by the Director, Office of Energy Research, Office of Basic Energy Sciences, Chemical Sciences Division of the U.S. Department of Energy under Contract No. W-7405-ENG-48.

Introduction

Since the discovery[1] and structural characterization[2,3] of ferrocene (η^5-$(C_5H_5)_2Fe$ or Cp_2Fe) in the early 1950's, at least one cyclopentadienyl derivative of every main group and transition metal as well as most f-block metals has been prepared and characterized.[4,5,6] A large number of monoalkyl- and monoaryl-substituted cyclopentadienyl metal compounds have also been prepared, but an extensive study of peralkylcyclopentadienyl metal compounds was not a practical possibility until recently, with the development of convenient and efficient synthetic routes to pentamethylcyclopentadiene and alkyltetramethylcyclopentadienes.[7-9] A number of studies have now appeared in the literature which demonstrate some dramatic differences in the structure and chemistry of cyclopentadienyl and pentaalklycyclopentadienyl metal compounds.[10-21] In general, these differences can be attributed to the relative steric bulk of the Me_5Cp^- ligand or to its lack of a ring carbon to hydrogen bond. The latter feature has proven especially useful in studies of early transition metal cyclopentadienyl derivatives where a common mode of reactivity involves insertion of the metal into a C-H bond of C_5H_5.[22-26] For example, attempts to prepare Cp_2Ti by Na/Hg reduction of Cp_2TiCl_2 or by treatment of $Cp_2Ti(Me)_2$ with H_2, yield instead a fulvalene-bridged dimer (I).[24] Other dimeric

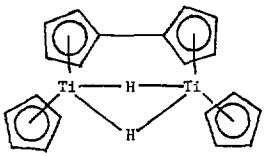

(I)

and polymeric forms of titanocene are known,[10] but the monomeric titanocene has not yet been isolated. In contrast, Bercaw found that $(Me_5Cp)_2Ti$ is obtained as a yellow-orange, crystalline solid when solvent is removed under vacuum from hydrocarbon solutions of the N_2-bridged, dimeric complex, $[(Me_5Cp)_2Ti]_2N_2$.[11] Infrared, NMR, cryoscopic molecular weight, and magnetic susceptibility data for $(Me_5Cp)_2Ti$ were consistent with its formulation as a monomeric, 14-electron decamethylmetallocene.

The steric effects of complete ring alkylation have proven particularly influential in the structure and chemistry of uranium(IV) and thorium(IV) cyclopentadienyl derivatives. Mononuclear complexes of these metals containing four Cp^- rings (Cp_4M; M=U,Th),[27,28] three Cp^- rings (Cp_3MCl; M=U,Th),[29,30] and one Cp^- ring ($CpMCl_3$(1,2-dimethoxyethane))[31] can be isolated, depending on reaction conditions and stoichiometry. The missing member of this series, Cp_2UCl_2, disproportionates to tris- and monocyclopentadienyl derivates in donor solvents[32] and an authentic Cp_2UCl_2 specimen has not yet been isolated.

With pentamethylcyclopentadienide or ethyltetramethylcyclopentadienide ($EtMe_4Cp^-$), monomeric uranium(IV) and thorium(IV) compounds containing one peralkylated ring, $((Me_5Cp)ThCl_3$,[6] $(EtMe_4Cp)UCp_2Cl)$,[33] and two peralkylated rings ($((Me_5Cp)_2MCl_2$; M=Th,U;[18] $(EtMe_4Cp)_2UCl_2)$[17] have been prepared, but mononuclear complexes containing three peralkylated rings have proven elusive.[6] Apparently, the steric requirements of two coordinated Me_5Cp^- rings prevent the attachment of a third ring in either a σ- or a π-fashion and the disproportionation route observed for Cp_2UCl_2 is thus blocked.

A third possible consequence of complete alkylation of the Cp^- ring is the effect of such a substitution on the electron donor/acceptor properties of the ring and the electronic structures of metal derivatives. A priori, the replacement of all the cyclopentadienyl hydrogens with electron-donating alkyl groups is expected to increase the basicity and π-donating capability of the ring, but this effect has not been explored in any detail. This dissertation describes an attempt to determine the existence and ramifications of such an effect through a systematic comparison of the chemistry and electronic structures of the first transition series metallocenes and the decamethylmetallocenes. [Note: in the following discussion, the terms "metallocene" and "decamethylmetallocene" refer only to those $[(\eta^5\text{-}C_5R_5)_2M]^{+/0/-}$ compounds (R=H, Me) that possess effective five-fold symmetry].

The isolation of the first transition series metallocenes, Cp_2V, $Cp_2Cr^{+/0}$, Cp_2Mn, $Cp_2Fe^{+/0}$, $Cp_2Co^{+/0}$, and $Cp_2Ni^{+/0}$ [34] has provided chemists a unique opportunity to examine the chemical and physical properties of a series of isostructural organometallic compounds which vary in their metal ion, orbital occupation, and oxidation state. In an effort to understand the nature of bonding in metallocenes, these complexes have been investigated using a number of physical methods, including magnetic susceptibility, electron paramagnetic resonance (EPR), nuclear magnetic resonance (NMR), UV-visible spectroscopy, and UV-photoelectron spectroscopy (UV-PES).[35,36] These studies reveal that the highest occupied molecular orbitals of the 15- through 20- electron metallocenes are strongly metal in character. This result, coupled with an

Figure 1. The molecular orbital diagram for ferrocene.[37]

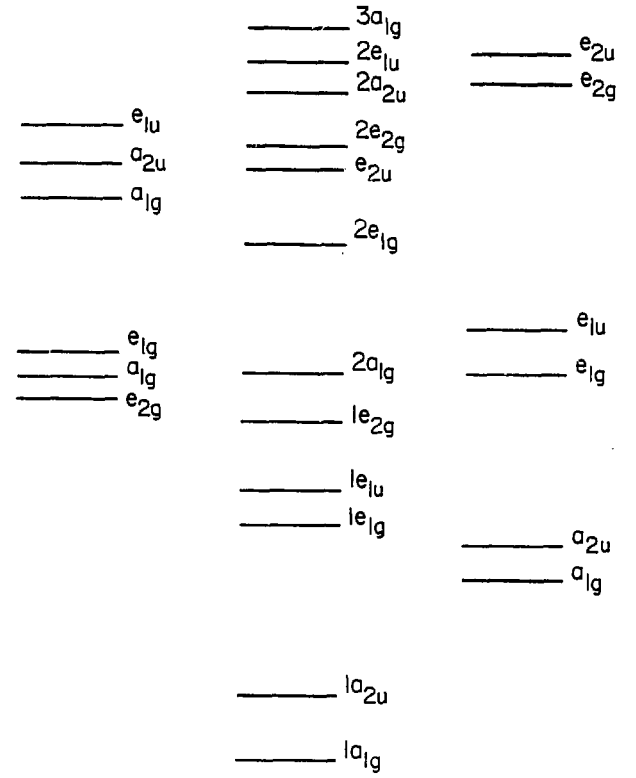

Metal orbitals

Ligand π-orbitals

XBL 798-2693

extended Hückel calculation, led Ballhausen and Gray to proprose the ferrocene molecular orbital diagram depicted in Figure 1.[37] The construction of this diagram utilizes the following basic symmetry considerations.

Under D_{5d} symmetry, the metal 3d orbitals are split into three irreducible representations: $a_{1g}(d_{z^2})$, $e_{1g}(d_{xz},d_{yz})$, and $e_{2g}(d_{xy}, d_{x^2-y^2})$. Similarly, the metal 4s and 4p orbitals transform to the a_{1g}, e_{1u}, and a_{2u} representations. A symmetry adapted linear combination of the ten ligand π-orbitals yields levels of a_{1g}, a_{2u}, e_{1g}, e_{2g}, and e_{2u} symmetry. The primary metal-ring bonding results from interaction of metal 3d and ring π-orbitals of e_{1g} symmetry. This overlap generates strongly bonding ($1e_{1g}$) and strongly antibonding ($2e_{1g}$) molecular orbitals. The overlap of the other metal 3d orbitals (e_{2g} and a_{1g}) with ligand π-orbitals is much weaker. Thus the molecular $2a_{1g}$ and $1e_{2g}$ levels retain a high degree of metal character. According to this model, the $2a_{1g}$ level is non-bonding and the $1e_{2g}$ level weakly bonding between the metal and rings. The eighteen valence electrons of ferrocene are accomodated by filling levels up to and including the $2a_{1g}$ level.

Ther reader is cautioned that the molecular orbital diagram shown in Figure 1 represents the results of only one of many calculations on the electronic structure of ferrocene.[35,38] There is general agreement that the principal metal-ring bonding in ferrocene is a consequence of metal and ring e_{1g} orbital overlap. Similarly, most calculations predict that the molecular $2a_{1g}$ level is essentially non-bonding. However, there remains some controversy regarding the ordering of the $2a_{1g}$, $1e_{2g}$ levels and the bonding

character of the $1e_{2g}$ orbital in ferrocene. In general, calculations of the extended Hückel type yield the orbital energy ordering as shown in Figure 1, $2a_{1g} > 1e_{2g}$, while self consistent field methods give the opposite result, $1e_{2g} > 2a_{1g}$. In the following discussions of metallocene and decamethylmetallocene electronic structure, we will use the ordering pattern $2a_{1g} > 1e_{1g}$, primarily because it provides the simplest interpretation of the d-d electronic transitions in 15-, 18-, and 20-electron metallocenes (see Chapter 2).

The bonding character of the $1e_{2g}$ orbital in ferrocene is difficult to evaluate. Experimentally, no spectroscopic probe can directly measure the "covalency" of the orbital. Most molecular orbital calculations on ferrocene indicate a weak, but non-neglible bonding contribution from the $1e_{2g}$ molecular orbital. This suggestion has been challenged experimentally by Hendrickson and Duggan.[48] Using a combination of infrared, Raman, Resonance Raman, and optical spectroscopic methods, they have proposed assignments for the low energy ring-metal-ring vibrational modes in ground state ferrocene ($^1A_{1g}[e_{2g}^4 a_{1g}^2]$), ground state ferricenium ion ($^2E_{2g}[e_{2g}^3 a_{1g}^2]$), and an excited state of the ferricenium ion ($^1E_{1u}(e_{1u}^3 e_{2g}^4 a_{1g}^2)$]. Finding that the energies of the symmetric and asymmetric ring-metal-ring modes are insensitive to both the oxidation state of ferrocene and the two different electronic configurations of the ferricenium ion, they conclude that the $1e_{2g}$ and $1e_{1u}$ levels are non-bonding with respect to the metal and rings.

The limitation of this analysis lies in its assumption that the oxidation of ferrocene does not perturb the energies of the other filled molecular orbitals. This may not be the case. Mössbauer

studies of ferrocene and ferricenium ion reveal only a small difference in the ^{57}Fe isomer shift of the two species ($\Delta I.S. \simeq 0.08$ mm sec^{-1})[39a] when compared to the more ionic Fe(II)/Fe(III) pair, $Fe(SO_4)_2 \cdot 6H_2O$, $Fe_2(SO_4)_3 \cdot 7H_2O$ ($\Delta I.S. \simeq 0.88$ mm sec^{-1}).[39b] This indicates that the charge on the Fe nucleus in ferrocene and ferricenium ion is very nearly the same. The result implies that either the $1e_{2g}$ orbital is a ligand localized one or that the one-electron oxidation of ferrocene is accompanied a substantial transfer of negative charge from the rings to the iron atom. The former conclusion is inconsistent with EPR studies of the ferricenium ion, which assign a high degree of metal character (ca. 90%) to the $1e_{2g}$ molecular orbital.[39c] The latter explanation is more reasonable and is supported by a number of self consistent field calculations on ferrocene and ferricenium ion.[38a,c,d] These studies find that the ferricenium $1e_{1g}$ level is depressed in energy relative to the $1e_{1g}$ level in ferrocene and that the $1e_{2g}$ orbital is more localized on the iron atom (and thus less covalent) in ferricenium ion than in ferrocene. In other words, the metal-ring π-bonding (e_{1g} orbital overlap) in ferrocene is enhanced by removal of an e_{2g} electron, but the bonding character of the $1e_{2g}$ orbital is diminished in the cation. So, although the results of Hendrickson and Duggan suggest that the metal-ring bond orders in ferrocene and ferricenium ion are very nearly identical, the individual orbital contributions to the metal-ring bonding in the two systems may well be quite different.

The molecular orbital scheme in Figure 1 has proven useful in accounting for the ground state electronic configurations and the 3d-3d electronic transitions of the other first row transition series

metallocenes.[35] Variations in the sizes and electronegativities of the transition metal ions will naturally lead to variations in the absolute energies of the molecular orbitals from complex to complex. However, our model retains the general feature that $E(2e_{1g}) > E(2a_{1g}) \sim E(1e_{2g})$ (E=energy) and that all three of these orbitals have substantial metal character. The ligand field parameters Δ_1 and Δ_2 are used to describe the separation of the $1e_{2g}$, $2a_{1g}$, and $2e_{1g}$ molecular orbitals (Figure 2; in subsequent discussions these levels will be referred to as the e_{2g}, a_{1g} and e_{1g} orbitals).

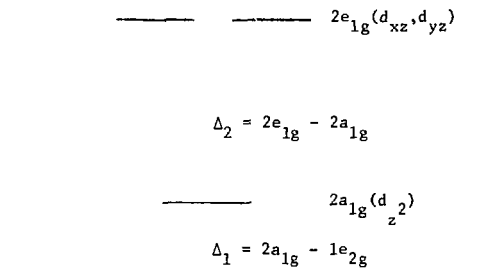

Figure 2

UV-photoelectron and UV-visible studies of first transition series metallocenes have established that Δ_1 is on the order of 4 to 7×10^3 cm^{-1} and Δ_2 is approximately $17 - 20 \times 10^3$ cm^{-1}.[40-42] Since Δ_1 is significantly smaller than the spin pairing energy, 15-electron metallocenes such as Cp_2V adopt a spin quartet ($^4A_{2g}; [e_{2g}^2 a_{1g}^1]$) rather than doublet ($^2E_{2g}[e_{2g}^3]$) electronic configuration. Δ_2 is

greater than the spin pairing energy so 16-, 17-, 18-, and 19-electron metallocenes exhibit low-spin configurations with S=1, 1/2, 0, and 1/2, respectively (Table I). The exception to this rule is the 17-electron complex manganocene, which has a high-spin, $^6A_{1g}$, ground state.[43] Manganocene is an anomally among the transition metal metallocenes in several other respects. It is a polymeric solid at room temperature,[44] is extraordinarily sensitive to air and water, possesses no known redox chemistry, and undergoes ring exchange reactions characteristic of predominantly ionic cyclopentadienides (e.g., NaCp, Cp_2Mg).[43] Appropriately, the following discussion of decamethylmetallocenes begins with investigations into the chemical, structural, and electronic properties of decamethylmanganocene. In Chapter 2, this theme is extended to include the decamethylmetallocenes of the other first transition series metals.

CHAPTER 1

Decamethylmanganocene Compounds

EXPERIMENTAL SECTION

General

Reagent grade tetrahydrofuran (THF) was predried with CaH_2. Hexane, pentane, toluene, 1,4-dioxane, 1,2-dimethoxyethane (DME), and THF were purified by distillation from sodium benzophenone ketyl and stored under argon. Acetone was purified by distillation from anhydrous K_2CO_3 and stored under argon. Spectroscopic grade acetonitrile was distilled from P_2O_5 and freeze-thaw degassed for optical and electrochemical studies. For EPR studies, spectroscopic grade toluene and methylcyclohexane were distilled from sodium and

Table I. Ground state electronic configurations of the first transition series metallocenes.[a]

Compound	Orbital Occupation	Electronic Configuration[b]
Cp_2V	$e_{2g}^2\ a_{1g}^1$	$^4A_{2g}$
$[Cp_2Cr]^+$	$e_{2g}^2\ a_{1g}^1$	$^4A_{2g}$
Cp_2Cr	$e_{2g}^3\ a_{1g}^1$	$^3E_{2g}$
Cp_2Mn	$e_{2g}^2\ a_{1g}^1\ e_{1g}^2$	$^6A_{1g}$
$[Cp_2Fe]^+$	$e_{2g}^3\ a_{1g}^2$	$^2E_{2g}$
Cp_2Fe	$e_{2g}^4\ a_{1g}^2$	$^1A_{1g}$
$[Cp_2Co]^+$	$e_{2g}^4\ a_{1g}^2$	$^1A_{1g}$
Cp_2Co	$e_{2g}^4\ a_{1g}^2\ e_{1g}^1$	$^2E_{1g}$
$[Cp_2Ni]^+$	$e_{2g}^4\ a_{1g}^2\ e_{1g}^1$	$^2E_{1g}$
Cp_2Ni	$e_{2g}^4\ a_{1g}^2\ e_{1g}^2$	$^3A_{2g}$

[a] From reference 35.

[b] Assuming D_{5d} molecular symmetry.

stored under argon. Deuterated solvents for NMR studies were vacuum distilled from the appropriate dessicant (CaH_2 for C_6D_6, P_2O_5 for CD_3CN, CaH_2 for THF-d_8), then freeze-thaw degassed and stored in a dry box under argon.

1,2,3,4,5-pentamethylcyclopentadiene,[7] sodium pentamethylcyclopentadienide,[10] $NiBr_2 \cdot 2DME$,[34] and decamethylferrocene[45] were prepared by literature procedures. Chromous acetate, $[Cr(OAc)_2]_2 \cdot 2H_2O$,[46] and commercially available $CoCl_2 \cdot 6H_2O$ were dehydrated by heating to 120°C in vacuo. Ferricenium hexafluorophosphate was prepared according to the procedure described by Pinsky.[46b] Ferricenium tetrafluoroborate was prepared by adding solid $NaBF_4$ (1 equilavent) to a filtered aqueous solution of $(Cp_2Fe)FeCl_4$ (Alfa). Upon cooling (5°C), crystalline $(Cp_2Fe)BF_4$ deposited. This was filtered in air, washed with water (10 ml) then THF (2 x 10 ml) and dried under vacuum. All other chemicals were reagent grade and used without further purification.

Air-sensitive solids were stored and manipulated in a Vacuum Atmospheres dry box equipped with a modified dry-train. Air-sensitive solutions and dry, deoxygenated solvents were transferred with 18-gauge stainless steel cannulae connected by polyethylene tubing (Clay-Adams, Intramedic, Fischer Scientific Co.). Unless otherwise noted, all reactions were carried out in dry, deoxygenated solvents under an argon atmosphere using standard Schlenk-tube techniques. Solutions for NMR, EPR, and optical studies were prepared and transferred to appropriate cells inside a dry box.

Infrared spectra were recorded with a Perkin Elmer 283 spectrophotometer which was calibrated with polystyrene. Samples were

prepared as KBr pelets or mulls (Nujol or Kel-F) between CsI plates. Proton NMR spectra and magnetic suceptibility measurements by the Evans NMR method were recorded on a Varian A-60 spectrometer. Proton decoupled ^{13}C NMR spectra were obtained at 25 MHz in the pulsed Fourier transform mode with a Nicolet TT-23 spectrometer. All chemical shifts are reported in ppm(δ) with reference to tetramethylsilane. Optical spectra were recorded on a Varian Associates Cary-17 with a nitrogen-purged sample compartment.

Bulk magnetic susceptibility measurements were made on a PAR Model 155 vibrating sample magnetometer calibrated with $HgCo(SCN)_4$ and equipped with a Janus Research Model 153 liquid helium dewar. Field strength was monitored with a George Associates rotating coil gaussmeter. Temperature was measured with a calibrated GaAs diode. Temperature was controlled with a thermostated resistance heater. Magnetic susceptibility data were corrected for contributions from the GaAs diode and the polyethylene sample containers by recording the field and temperature dependence of the empty containers just prior to filling them with sample material.

X-band EPR spectra of decamethylmetallocenes in frozen toluene or methylcyclohexane solution (~0.1M) or diluted in diagmagnetic decamethylmetallocenes at 10-15 K were obtained using a Varian E-12 spectrometer employing an Air Products Helitran cooling system mounted in the Varian room temperature cavity. The cavity frequency was measured with a Hewlett-Packard transfer oscillator and frequency counter, and the magnetic field with a proton NMR gaussmeter.

Cyclic voltammograms were recorded in the three-electrode configuration with a platinum disc working electrode, a platinum

wire auxiliary electrode and a $Ag/AgNO_3$ (CH_3CN) reference electrode inside an inert atmosphere box. All potentials were referenced to the saturated calomel electrode (SCE) by measuring the ferrocene/ferricenium couple under identical conditions. Triangular waves were generated by the Princeton Applied Research (PAR) 175 Programmer in conjunction with the PAR 173 Potentiostat, and current-voltage curves were recorded on a Houston Omnigraphics 2000 x-y recorder. For controlled potential coulometry, a platinum basket working electrode was employed, and the current integrated with the PAR 179 Digital Coulometer.

Mass spectra were recorded on an AEI-MS 12 mass spectrometer equipped with a direct inlet system. Elemental analyses were performed by the Microanalytical Laboratory of the University of California, Berkeley. Melting points were determined on a Thomas-Hoover Unimelt apparatus and are uncorrected.

Preparation of Complexes

Bis(pentamethylcyclopentadienyl)manganese(II),

1,2,3,4-pentamethylcyclopentadiene (2.05g, 15.1 mmol) in THF (150 mL) was cooled to -78°C (dry ice-ethanol) then treated with n-butyl lithium (6.3 mL, 2.4M in hexane, 15.1 mmol) added with a syringe. Upon warming to room temperature, white lithium pentamethylcyclopentadienide precipitated from a bright yellow solution. The stirred suspension was cooled to -78°C and anhydrous $MnCl_2$ (1.34g, 10.6 mmol) added against an N_2 counterstream. The mixture was slowly warmed to 40°C (ca 1 hour) then stirred an additional hour to produce a clear orange solution. Solvent was removed in vacuo and the crude orange-brown solid sublimed (100°C/10^{-5} torr) to yield the product as an air sensitive red-orange solid (1.87g, 76%). Crystallization from hexane gave orange prisms. Anal. Calcd. for $C_{20}H_{30}Mn$: C, 73.82; H, 9.29. Found: C, 73.96; H, 9.18. m.p. 292°C. ^1H NMR (60 MHz, C_6D_6) δ ~ 4.7(s). linewidth 200 Hz at half height; 320 K. Infrared (Nujol, Halocarbon Mulls): 2980 m, 2940 m, 2895 s, 2850 m, 2710 w, 1470 m, 1448 m, 1[illegible] m, 1373 ms, 1355 w, 1065 m, 1023 s, 722 w, 588 w, 445 m, 361 m cm^{-1}. Mass Spectrum (70 eV) [m/e (relative abundance)]: $(P+1)^+$, 326(8), P^+, 325(38), 189(7), 137(12), 136(67), 135(27), 133(8), 122(11), 121(100), 120(11), 119(53), 117(7), 115(6), 108(10), 107(11), 106(11), 105(51), 103(8), 94(6), 93(28), 91(41), 83(5), 81(6), 79(6), 78(7), 77(22), 71(6), 69(7), 65(12), 57(11), 55(16), 53(13), 51(9).

Sodium bis(pentamethylcyclopentadienyl)manganate(I).

Naphthalene (0.53g, 4.12 mmol) in THF (30 mL) was stirred over freshly cut sodium (0.12g, 5.22 mmol) for 1 hour. The resulting solution of sodium naphthalide was added rapidly through a cannula to solid $(Me_5Cp)_2Mn$ (1.34g, 4.12 mmol) producing a deep red solution. After stirring at room temperature for 15 minutes, solvent was removed under reduced pressure and the resulting orange powder suspended in hexane (40 mL), filtered, washed with hexane, (2 x 20 mL) and dried *in vacuo* to yield $Na[(Me_5Cp)_2Mn]$ as an orange pyrophoric powder (1.36g, 95%). Recrystallization from THF/hexane afforded bright orange needles which disintegrated to an orange powder upon drying. Anal. Calcd. for $C_{20}H_{30}MnNa$: C, 68.95; H, 8.68. Found: C, 68.19; H, 8.72. ^1H NMR (60 MHz, THF-d_8) δ 1.87(s). $\{^1H\}^{13}C$ NMR: (25 MHz, THF-d_8) δ 8.54(s), 72.4(s). Infrared (Nujol mull, KBr pellet): 2950 s, 2860 s, 2730 m, 2710 w, 1450 s, 1400 m, 1380 s, 1165 w, 1067 w, 1030 s, 722 m, 580 w, 498 s, 389 m, 285 s, 250 m cm^{-1}.

Bis(pentamethylcyclopentadienyl)manganese(III) Hexafluorophosphate.

A mixture of $(Me_5Cp)_2Mn$ (1.41g, 4.3 mmol) and $(Cp_2Fe)PF_6$ (1.35g, 4.0 mmol) in acetone (50 mL) was stirred for 1 hour at room temperature to give a cherry red solution. After removal of solvent under reduced pressure, the product was suspended in hexane (20 mL), filtered and washed with additional hexane until washings were colorless (3 x 20 mL). Drying *in vacuo* yielded $[(Me_5Cp)_2Mn]PF_6$ as dark red microcrystals (1.6g, 85%). Dark red prisms were obtained by recrystallization from acetone/hexane. $[(Me_5Cp)_2Mn]PF_6$ in acetone or acetonitrile solution is slowly hydrolyzed by water but the solid

may be handled in air for short periods of time. Anal. Calcd. for $C_{20}H_{30}MnPF_6$: C, 51.07; H, 6.43; P, 6.58. Found: C, 51.21; H, 6.40; P, 6.39. ^1H NMR (60 MHz $(CD_3)_2CO$) δ 3.13(s), linewidth = 18 Hz at 310K. Infrared (Nujol, Halocarbon mull): 2991 m, 2963 m, 2921 m, 1474 s, 1423 m, 1393 vs, 1069 m, 1022 s, 874 s, 840 vs, 722 w, 589 w, 540 vs, 505 m, 439 m, 230 w cm^{-1}.

Bis(pentamethylcyclopentadienyl)iron(III) Hexafluorophosphate.

In air, $FeCl_3$ (0.2g, 1.23 mmol) was added to a solution of $(Me_5Cp)_2Fe$ (0.52g, 1.61 mmol) in THF (20 mL) to give a blue-green solution of $[(Me_5Cp)_2Fe]^+$. After stirring for 30 minutes at room temperature, solid NH_4PF_6 (0.5g, 3 mmol) was added and stirring was continued for an additional 30 minutes. The resulting solid was filtered, washed with THF (2 x 10 mL) and H_2O (2 x 10 mL) then dried in vacuo to yield $[(Me_5Cp)_2Fe]PF_6$ as air stable blue-green microcrystals (0.52g, 90% based on $FeCl_3$). Recrystallization from acetone gave blue-green prisms. Anal. Calcd. for $C_{20}H_{30}FePF_6$: C, 50.97; H, 6.42. Found: C, 51.12; H, 6.43. Infrared (Nujol, Halocarbon mulls) 2990 m, 2960 s, 2922 s, 2860 s, 1470 s, 1458 sh, 1420 m, 1390 s, 1380 s, 1072 m, 1023 s, 878 s, 843 vs, 778 w, 722 vw, 590 w, 558 vs, 532 m, 450 m, 348 m cm^{-1}. These values are in agreement with previously reported IR spectra of $[(Me_5Cp)_2Fe]PF_6$.[48]

RESULTS AND DISCUSSION

Synthesis and Characterization

Decamethylmanganocene [$(Me_5Cp)_2Mn$] was prepared in high yield *via* the reaction of anhydrous $MnCl_2$ with $(Me_5Cp)Li$ in THF. The crystalline solid decomposes in air and solutions of the complex are extremely oxygen sensitive. In THF solution, $(Me_5Cp)_2Mn$ does not react with $FeCl_2$ and is hydrolyzed only slowly (over a period of hours) by water. This behavior is in marked contrast to that of Cp_2Mn and $(MeCp)_2Mn$, both of which are pyrophoric solids, are instantly hydrolyzed by water and react rapidly with $FeCl_2$ in THF to yield the corresponding ferrocenes.[43,49]

As both the thermodynamic and kinetic stability of a metal complex is dependent on spin state, it is worth noting that Cp_2Mn and $(MeCp)_2Mn$ possess thermally accessible high-spin ($^6A_{1g}$) electronic configurations, while $(Me_5Cp)_2Mn$ exists solely in a low-spin ($^2E_{2g}$) state (*vide infra*). In contrast to the high-spin d^5 case, the low-spin d^5 configuration possesses substantial crystal field stabilization[50] with attendant increase in ring-metal bond strength. The observation of shorter (by nearly 0.3 Å) metal to ring carbon distances in the low-spin manganocenes,[51,47c] is consistent with these predictions.

The contrasting reactivity of high- and low-spin manganocenes parallels the situation observed in Mn(II) coordination chemistry. No crystal field activation energy for ligand displacement is expected for high-spin octahedral d^5 systems and accordingly, high-spin Mn(II) complexes, such as $Mn(1,10\text{-phenanthroline})_3^{2+}$, are notoriously labile.[52] In the low-spin d^5 case, a significant activation energy prevails and low-spin species such as $Mn(CN)_6^{4-}$ are relatively

inert.[52,53] While $(Me_5Cp)_2Mn$ is relatively inert towards ring loss and hydrolysis, it does undergo reversible one-electron oxidation as well as reduction to yield isolable low-spin 16- and 18-electron species in a fashion similar to $Mn(CN)_6^{4-}$.[54,55]

Manganocene is unique among transition metal metallocenes in that no cationic derivative has been isolated. Decamethylmanganocene, however, is readily oxidized by $(Cp_2Fe)^+$ in acetone to yield the dark red complex $[(Me_5Cp)_2Mn]^+$. The cyclic voltammogram of $[(Me_5Cp)_2Mn]PF_6$ (Figure 3) shows that this compound is reduced in two reversible one-electron steps at -0.56 and -2.17 V vs. SCE, with peak separations of 60 and 80 mV, respectively. The latter separation exceeds the theoretical value of 59 mV[56] because of its proximity to the cathodic wave of CH_3CN. Controlled potential coulometry on the first reduction establishes that n=0.98±.02 verifying the one-electron nature of the reduction. In acetone solution $[(Me_5Cp)_2Mn]^+$ is hydrolyzed slowly by H_2O but rapidly in the presence of strong acid (CF_3CO_2H).

As the cyclic voltammogram in Figure 3 suggests, $(Me_5Cp)_2Mn$ may also be reduced by one electron to an anionic derivative. Treatment of $(Me_5Cp)_2Mn$ with sodium naphthalide in THF gives a solution of $Na[(Me_5Cp)_2Mn]$,[57] which is isolated as an orange, pyrophoric powder soluble in THF, 1,2-dimethoxyethane, and N,N,N',N'-tetramethylethylenediamine, but insoluble in aromatic and aliphatic hydrocarbon solvents. The difficulty in obtaining accurate analytical results for $Na[(Me_5Cp)_2Mn]$ is probably related to extreme sensitivity to air. The electrochemical reductions of Cp_2V, Cp_2Cr, Cp_2Co, and Cp_2Ni have been reported but the reduced species were neither isolated nor characterized in solution.[58] Therefore, $Na[(Me_5Cp)_2Mn]$ represents the

Figure 3. Cyclic voltammogram of $[(Me_5Cp)_2Mn]PF_6$ in CH_3CN on Pt disc electrode with 0.1M $[(\underline{n}\text{-butyl})_4N]BF_4$ electrolyte. Scan rate = 100 mV sec^{-1}.

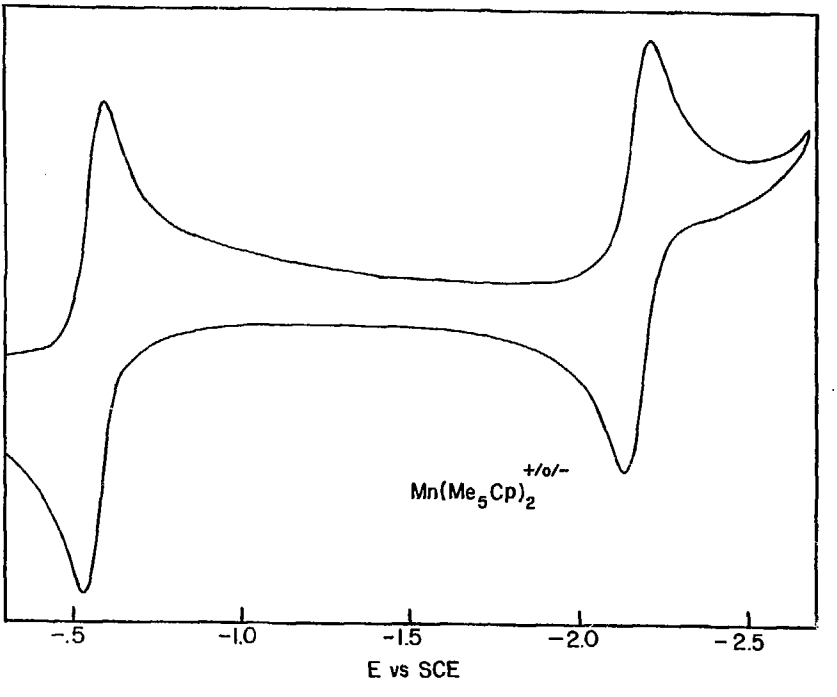

XBL 786-4047

first example of a stable, isolable metallocene anion. The anion reacts with CH_3CN, $(CH_3)_2CO$, MeI, and H_2O to give $(Me_5Cp)_2Mn$ in high yield. There is no evidence (infrared) for the formation of $(Me_5Cp)_2$-MnH or $(Me_5Cp)_2MnCH_3$ in these reactions. The complex also reacts with $FeCl_2$ in THF, again to give $(Me_5Cp)_2Mn$ with no detectable amount of $(Me_5Cp)_2Fe$.

An Evans NMR method[59] measurement shows that $Na[(Me_5Cp)_2Mn]$ is diamagnetic in THF solution. The ^1H and proton decoupled ^{13}C NMR spectra of the anion are similar to those of other diamagnetic Me_5Cp^- compounds (see Chapter 2) so we conclude that the anion is a planar 18-electron metallocene, isoelectronic with $(Me_5Cp)_2Fe$.

An X-ray crystallographic study has verified the planar metallocene structure for $(Me_5Cp)_2M$[47c] and $[(Me_5Cp)_2M]PF_6$[60] (M = Mn,Fe) in the solid state. Infrared spectra of the neutral complexes $(Me_5Cp)_2Mn$ and $(Me_5Cp)_2Fe$ are superimposable in the region 900 cm^{-1} to 4000 cm^{-1} with characteristic absorptions between 2800 and 3000 cm^{-1} (4 bands), 1500 and 1350 cm^{-1} (5 bands) and 1000 to 1100 cm^{-1} (2 bands). Spectra of $[(Me_5Cp)_2Mn]PF_6$, $[(Me_5Cp)_2Fe]PF_6$, and $Na[(Me_5Cp)_2Mn]$ are similar, but more poorly resolved. These absorptions do not vary significantly in this series of compounds so they probably represent primarily ligand vibrational modes for η^5-bound Me_5Cp^-. Similarly, the reversibility observed in the cyclic voltammogram of $(Me_5Cp)_2Mn$ is consistent with simple oxidation-reduction reactions in a series of complexes retaining the D_{5d} or D_{5h} metallocene structure.

Magnetic Susceptibility

The metallocene molecular orbital energy level diagram allows the possibility of low-spin ($^2A_{1g}[e_{2g}^4 a_{1g}^1]$, $^2E_{2g}[e_{2g}^3 a_{1g}^2]$) and high-spin ($^6A_{1g}[e_{2g}^2 a_{1g}^1 e_{1g}^2]$) ground states for a d^5 system such as Cp_2Mn. Magnetic susceptibility studies have shown that the spin state of manganocene is sensitive to temperature, environment, and methyl substituents.

Solid Cp_2Mn undergoes a phase transition at 432 K from its low-temperature brown form to a pink form. The pink form displays normal Curie behavior for an S = 5 2 molecule, as does Cp_2Mn in benzene or ether solution or diluted in Cp_2Mg. Below the phase transition temperature, however, the susceptibility of Cp_2Mn shows a temperature dependence suggestive of antiferromagnetism.[43] Bunder and Weiss's recent crystallographic study of the brown form showed that it does not consist of discrete Cp_2Mn molecules, but rather exhibits a polymeric zig-zag chain structure.[44] Crystalline $(MeCp)_2Mn$ is also apparently antiferromagnetic.[61] Tetrahydrofuran solutions of $(MeCp)_2Mn$ obey the Curie-Weiss law for an S = 5/2 system,[61] but these data may pertain to the solvated complex, $(MeCp)_2Mn \cdot 2THF$.[62] Rettig and co-workers demonstrated that the anomalous magnetic behavior of $(MeCp)_2Mn$ in toluene solution is due to a spin-state equilibirum with $\Delta H° = -1.8 \pm 0.1$ kcal mole^{-1} and $\Delta S° = -5.8 \pm 0.6$ e.u. for the high- to low-spin conversion in toluene.[62]

The magnetic susceptibility measurements on solid $(Me_5Cp)_2Mn$, $[(Me_5Cp)_2Fe]PF_6$, and $[(Me_5Cp)_2Mn]PF_6$ indicate Curie-Weiss behavior ($\chi_m = C/(T-\theta)$) in each case. The results of these experiments, and

Table II. Magnetic Susceptibility Data for Decamethylmetallocenes.

			SOLID		SOLUTION	
Molecule	C	θ^b	$\mu_{eff}{}^a$	Temperature Range[b]	$\mu_{eff}{}^a$	Temperature[b]
$(Me_5Cp)_2Mn$	0.59	0	2.17 ± .1	4.2 to 117	1.97 ± .1	313[c]
$[(Me_5Cp)_2Fe]PF_6$	0.63	0	2.25 ± .1	4.2 to 70	2.40 ± .1	310[d]
$[(Me_5Cp)_2Mn]PF_6$	1.18	-4	3.07 ± .1	4.2 to 65	2.90 ± .1	310[d]

a) Values in Bohr magnetons.

b) Temperatures in degrees K.

c) Measured in toluene solution.

d) Measured in acetone solution.

the solution magnetic moments as determined by the Evans NMR method,[59] are summarized in Table II. For solid $(Me_5Cp)_2Mn$ our data reveal a temperature independent moment of $2.17\mu_B$ up to 117 K, in agreement with the solution moment measurement at 313 K. These data are consistent with the formulation of a low-spin doublet ground state for $(Me_5Cp)_2Mn$; the temperature independence of the moment indicates that thermal population of the $^6A_{1g}$ state is negligible up to 313K. A recent UV-photoelectron study of $(Me_5Cp)_2Mn$ shows that the molecule is low-spin in the gas-phase as well. No evidence was found for a high-spin form up to 384 K.[63] A magnetic moment of $2.26\mu_B$ is obtained for the isoelectronic molecule, $[(Me_5Cp)_2Fe]PF_6$. Both these values are close to the magnetic moment of low-spin $(MeCp)_2Mn$, ($\mu_{eff} = 1.98\ _B$ at 15K) calculated from EPR spectral data.[62,64]

The magnetic moments of the low-spin d^5 metallocenes are significantly larger than the spin-only value for an S = 1/2 molecule ($1.78\mu_B$). This suggests that the ground state of these molecules is the orbitally degenerate $^2E_{2g}$ configuration rather than the nondegenerate $^2A_{1g}$ configuration. A spin-only moment is expected (and found) for metallocenes with nondegenerate electronic configurations.[65] However, significant orbital contributions to the moment are expected for metallocenes with an orbitally degenerate ground state. For $^2E_{2g}$ ground state metallocenes, Warren's ligand field calculations anticipate that such contributions will result in modestly temperature dependent magnetic moments ranging from 3.0 to $3.1\mu_B$ (30 to 300K).[65] The magnetic parameters of metallocenes with orbitally degenerate ground states are also subject to the

influence of low symmetry distortions from pure axial symmetry and delocalization of the unpaired electron over ligand π-orbitals. Warren calculates that the effects of a static C_{2v} distortion and an increase in the covalency of the e_{2g} orbital will serve to quench the orbital angular momentum and yield moments that approach the spin-only value.[65] Our magnetic susceptibility data for the 17-electron decamethylmetallocenes are thus well within the range expected for a $^2E_{2g}$ ground state assignment. This assignment is confirmed by EPR and UV-PES studies of $(Me_5Cp)Mn$[63] and $[(MeCp)_2Fe]PF_6$[48,63](see below).

Like Cp_2Cr, $[(Me_5Cp)_2Mn]PF_6$ is a 16-electron metallocene with three possible ground state electronic configurations: $^3A_{2g}[e_{2g}^2a_{1g}^2]$, $^3E_{2g}[e_{2g}^3a_{1g}^1]$, and $^5E_{1g}[e_{2g}^2a_{1g}^1e_{1g}^1]$. Warren and Gordon recently reported moments of 3.23 and 3.17μ_B for Cp_2Cr and $(MeCp)_2Cr$, respectively.[66] These values were consistent with an S=1 spin system ($\mu_{spin\ only} = 2.83\mu_B$) with significant orbital contributions to the moment. On the basis of this evidence and the results of UV-photoelectron studies,[42b] the orbitally degenerate $^3E_{2g}$ ground state has been assigned to the chromocenes.[66] Our magnetic data for $[(Me_5Cp)_2Mn]PF_6$ are also consistent with a spin triplet configuration; thus this complex is a rare example of low-spin Mn(III). The solution and solid state moments are only slightly greater than the spin-only value for an S = 1 system, hence it is not possible to assign unambiguously either a $^3E_{2g}$ or $^3A_{2g}$ configuration from magnetic susceptibility data. EPR spectroscopy does not assist us in this choice of ground states: $[(Me_5Cp)_2Mn]PF_6$ diluted in $[(Me_5Cp)_2Co)]PF_6$ gives no EPR signal at either 12 K or 298 K. However, Green's

UV-photoelectron study of $(Me_5Cp)_2Mn$ provides definitive proof that the ground state of $[(Me_5Cp)_2Mn]^+$ in the gas-phase is the orbitally degenerate $^3E_{2g}$ electronic configuration.[63]

EPR

EPR investigations confirm the dependence of the manganocene electronic structure on methyl substituents and environment noted in magnetic susceptibility studies. Manganocene in toluene or methylcyclohexane glasses and diluted in Cp_2Mg exhibits EPR spectra characteristic of the high-spin $^6A_{1g}$ configuration.[62,64] When Cp_2Mn is diluted in Cp_2Fe, Cp_2Ru, or Cp_2Os spectra consistent with the $^2E_{2g}$ configuration found in ferricenium systems[48] are observed.[64,68] As Ammeter has indicated, the ring to metal distance of Cp_2Mg and high-spin Cp_2Mn are comparable so the high-spin form is easily accommodated in such a lattice. The other metallocene hosts have much shorter ring to metal distances, thereby favoring the low-spin form of Cp_2Mn[68] (which is expected to have a distinctly shorter ring-metal distance than the high-spin form). For $(MeCp)_2Mn$, spectra characteristic of the $^2E_{2g}$ state are observed at 4.2 K in methylcyclohexane or toluene glasses and in host lattices of $(MeCp)_2Fe$ and $(MeCp)_2Mg$.[64,68]

We have measured the low-temperature EPR spectra of $(Me_5Cp)_2Mn$ both in toluene and methylcyclohexane glasses and diluted in $(Me_5Cp)_2Fe$. Our results together with earlier results on low-spin manganocenes are listed in Table III. As has been found for ferricenium derivatives[48,68] and low-spin Cp_2Mn and $(MeCp)_2Mn$,[64,68] the $(Me_5Cp)_2Mn$ g-values are anisotropic ($g_{||} \neq g_{\perp}$), deviate substantially

from 2.0, and are sensitive to changes in the diamagnetic host lattice. These data are not consistent with a $^2A_{1g}[e_{2g}^4 a_{1g}^1]$ ground state electronic configuration for which an isotropic g-tensor near g=2 is expected (this expectation is realized in the case of the bis-arene complex $[(\eta^6\text{-}C_6H_6)_2Cr]^+$ which possesses a $^2A_{1g}$ ground state).[35] Our spectra can, however, be analyzed within the framework of the orbitally degenerate $^2E_{2g}$ electronic configuration.

As was noted in the magnetic susceptibility section, the magnetic parameters of metallocenes with orbitally degenerate ground states are subject to the effects of orbital angular momentum, deviations from five-fold symmetry, and delocalization of the unpaired electron over ligand π-orbitals. Under pure axial symmetry, the g-values for a $^2E_{2g}$ metallocene are given by $g_\perp=0$, $g_{||}=2(2k'+1)$.[69] Here, k' is the orbital reduction factor, a measure of the delocalization of the unpaired e_{2g} electron over ligand orbitals. In the limits of no e_{2g} "covalency", k'=1 and $g_{||}=6$. With increasing delocalization, k' tends towards 0 and $g_{||}$ approaches 2.0. These results are not consistent with the observed spectra since they predict $g_\perp=0$ for any value of k'.

Maki and Berry have developed expressions for the g-values of $^2E_{2g}$ metallocenes which take into account the effects of covalency and distortions from axial symmetry.[69] According to their theory, the g-values for the $^2E_{2g}$ state are given by:

$$g_{||} = 2 + 4k'(1 - \zeta^2)/(1 + \zeta^2)$$

$$g_\perp = 4\zeta/(1 + \zeta^2)$$

Table III. EPR Results for the Low-Spin Manganocene Type Compounds

COMPOUND	$g_{\parallel}$	$g_{\perp}$	k'	ζ (cm^{-1})	$\lvert\delta\rvert$ (cm^{-1})	$2(\zeta^2 + \delta^2)^{1/2}$ (cm^{-1})	REFERENCE
$(Me_5Cp)_2Mn$ in toluene glass 12°K	3.26 ± .01	1.68 ± .02	.58	177	274	652	This work
$(Me_5Cp)_2Mn$ in methylcyclohexane glass 12°K	3.36 ± .01	1.42 ± .04	.48	147	148	417	This work
$(Me_5Cp)_2Mn$ in $(Me_5Cp)_2Fe$ 12°K	3.508 ± .004[b]	1.17 ± .01	.47	142	102	350	This work
Cp_2Mn in Cp_2Fe at 4.2°K	3.519 ± .004	1.222 ± .010	.48	146[a]	113[a]	369	63
Cp_2Mn in Cp_2Ru at 4.2°K	3.548 ± .004	1.069 ± .020	.46	140[a]	88[a]	330	68
Cp_2Mn in Cp_2Os at 4.2°K	3.534 ± .004	1.126 ± .01	.46	142[a]	96[a]	342	68
$(MeCp)_2Mn$ in toluene glass at 4.2°K	2.887	1.900	.71	217	659	1388	62
$(MeCp)_2Mn$ in methylcyclohexane glass at 4.2°K	2.909	1.893	.70	215	630	1331	62
$(MeCp)_2Mn$ in $(MeCp)_2Mg$ at 4.2°K	3.00 ± .02	1.889 ± .002	.76	232[a]	667[a]	1412	63
$(MeCp)_2Mn$ in $(MeCp)_2Fe$ at 4.2°K	3.06 ± .02	1.850 ± .002	.70	213[a]	518[a]	1120	63

a) Those values have been recalculated using the Kuki and Berry theory.
b) ^{55}Mn hyperfine coupling observed. $A_{\parallel} = 61.9 \pm .3 \times 10^{-4} cm^{-1}$; $A_{\perp}$ not resolved.

XBL 791-8054

$$\zeta = \left(\frac{\delta}{\zeta}\right) / \left\{1 + \left\{1 + \frac{\delta}{\zeta}^{2}\right\}^{1/2}\right\} \quad ,$$

Here k' is the orbital reduction factor and δ is introduced as a low symmetry distortion parameter, a measure of the departure from axial symmetry. Also, $\zeta = k'\zeta_0$ where ζ_0 is the spin-orbit coupling constant for the bare metal ion. Note that in the limit of no covalency (k'=1) and pure axial symmetry ($\delta = 0$ cm^{-1}), $g_{\perp}=0$ and $g_{\parallel}= 6$, as before. As the effects of geometric distortions from axial symmetry and e_{2g} electron delocalization become important (i.e. $k' < 1$; $\delta > 0$) the g-values will tend towards 2. We have used the Maki and Berry theory to calculate the k' and δ parameter values for $(Me_5Cp)_2Mn$ and other low-spin manganocene compounds (Table III). The parameter values are obtained explicitly from the equations using the experimental EPR data and an assumed value of ζ_0. We follow the suggestion of Switzer, et. al. Using $\zeta_0 = 305$ cm^{-1} for the bare metal ion, Mn^{+1}.[62]

The k' and δ values obtained for $(Me_5Cp)_2Mn$ and Cp_2Mn in a variety of hosts are quite similar but differ significantly from those determined for $(MeCp)_2Mn$. The parameter δ is much larger for $(MeCp)_2Mn$ which may be due to the relatively low symmetry of this molecule. The k' values are also smaller in the more symmetric manganocenes, implying a greater delocalization of the unpaired electron in $(Me_5Cp)_2Mn$ and Cp_2Mn than in $(MeCp)_2Mn$. The reduction of k' can result from either increased covalency or dynamic Jahn-Teller effects.[68] The low k' values observed for Cp_2Mn relative to $(MeCp)_2Mn$ were attributed to increased dynamic Jahn-Teller coupling

in Cp_2Mn.[68] The crystal structure of $(Me_5Cp)_2Mn$ revealed static distortions involving metal-ring carbon and ring carbon-ring carbon distances at room temperature, but no evidence was found for dynamic Jahn-Teller distortions.[47c] If this result holds for $(Me_5Cp)_2Mn$ in the matrices employed in the EPR studies, then the low k' values must result from increased covalency in the $(Me_5Cp)_2Mn$ system.

It is interesting to compare the EPR spectral data and derived parameter values of $(Me_5Cp)_2Mn$ with those of the isoelectronic complex $[(Me_5Cp)_2Fe]^+$. Hendrickson and Duggan have measured the EPR spectra of neat samples of this cation both as the PF_6^- salt, (1) and as the trichloroacetate salt (with two trichloroacetic acid molecules per cation in the unit cell, 2).[48] The spectra of 1 and 2 exhibit $g_{||}:g_{\perp}$ resonances at 4.433:1.350 and 4.37:1.26, respectively (X-band; 12K). The $g_{\perp}$ values are close to those found for $(Me_5Cp)_2Mn$, but the $g_{||}$ values are substantially larger for the iron complex. Calculation of the k' and δ values using the Maki and Berry expressions (with $\zeta_0 = 405\ cm^{-1}$ for Fe(II)[69]) gives k' = 0.82; $\delta = 305\ cm^{-1}$ for 1 and k' = 0.76; $\delta = 250\ cm^{-1}$ for 2. The distortion parameters are rather small and are in general similar to the values found for $(Me_5Cp)_2Mn$. However, the k' values for $[(Me_5Cp_2)Fe]^+$ are much larger than those determined for $(Me_5Cp)_2Mn$. As was implied earlier, the parameter k' is related to the percent metal character of the orbital involved. If the latter quantity is defined as k, then the approximate relationship $k' \approx k^2$ is expected.[69] We thus find that the e_{2g} orbital is localized on the metal atom to an extent of 70-75% in $(Me_5Cp)_2Mn$ and 87-91% in $[(Me_5Cp)_2Fe]^+$. These

numbers should be viewed in a relative rather than an absolute sense because the relationship between k' and k is only an approximate one. Nonetheless, it appears that the e_{2g} orbital has a stronger bonding character in $(Me_5Cp)_2Mn$ than in $[(Me_5Cp)_2Fe]^+$. In the absence of reliable calculations on these two species, it is attractive to postulate that the spatial expansion of the metal 3d orbitals in the neutral Mn complex is greater than in the cationic Fe derivative, affording better metal-ring e_{2g} orbital overlap.

Structures

Structural studies of manganocenes have demonstrated the dependence of the metal-to-ring carbon distance [R(M-C)] on the spin state of the molecules. Bünder and Weiss's recent X-ray crystallographic study of Cp_2Mn showed that it is polymeric in its low temperature brown form.[44] At 432 K, Cp_2Mn undergoes a phase transition to a pink form which is isomorphous with the other first transition series metallocenes (space group = $P2_{1/c}$). Manganocene is presumably monomeric in this phase, but its high volatility at such temperatures precluded a complete structure determination.[44]

Haaland and co-workers have determined the structure of Cp_2Mn in the gas-phase by electron diffraction. In the vapor it is a monomeric, D_{5h} metallocene with an R(M-C) of 2.385(3) Å.[70] This is an exceptionally long metal to ring bond when compared to other metallocenes of the first transition series (Table IV), but is close to the R(M-C) determined for Cp_2Mg, 2.339(14) Å in the gas phase.[71]

A gas phase electron diffraction study of $(MeCp)_2Mn$ revealed the presence of two metallocene species in the vapor at 373 K, with

average R(M-C)s of 2.433(8) and 2.144(12) Å.[72] Comparison of these bond lengths with the bond length observed in the high-spin Cp_2Mn led to the conclusion that the former distance represents high-spin ($^6A_{1g}$) and the latter, low spin ($^2E_{2g}$) $(MeCp)_2Mn$. This assignment is supported by single crystal X-ray crystallography and gas phase electron diffraction studies of the rigorously low-spin derivative, $(Me_5Cp)_2Mn$.[47c,47d]

Crystalline decamethylmanganocene (space group = $C_{2/C}$) consists of discrete $(Me_5Cp)_2Mn$ molecules whose rings are in a staggered configuration (Figures 4 and 5). The average R(Mn-C) is 2.114(2) Å, about 0.3 Å shorter than the corresponding distance in high-spin $(MeCp)_2Mn$ and Cp_2Mn. The value is, however, very close to that determined for low-spin $(MeCp)_2Mn$. The contraction of the metal-ring distance in low-spin manganocenes can be rationalized on the basis of the molecular orbital diagram for high- and low-spin metallocene d^5 systems. In the $^6A_{1g}$ configuration, 3 electrons occupy the bonding e_{2g} and non-bonding a_{1g} levels and 2 electrons occupy the antibonding e_{1g} level. In the $^2E_{2g}$ configuration, all five 3d electrons reside in the e_{2g} and a_{1g} levels, leaving the antibonding e_{1g} level vacant. A net increase in the formal metal-ring bond order is expected, and the foreshortening of the bond is not surprising. Haaland has advanced similar arguments to explain the relative metal-to-ring distances observed in neutral metallocenes of the first transition series.[72,73] Assuming that the e_{2g} and a_{1g} levels are bonding between metal atom and rings while the e_{1g} level is antibonding, Haaland defines the "metallocene electron imbalance", n, as the sum of the number of electrons in the e_{1g}

Figure 4. Packing diagram of $(Me_5Cp)_2Mn$ with the unit cell edges shown. b is horizontal, c is vertical, while a is into the paper.

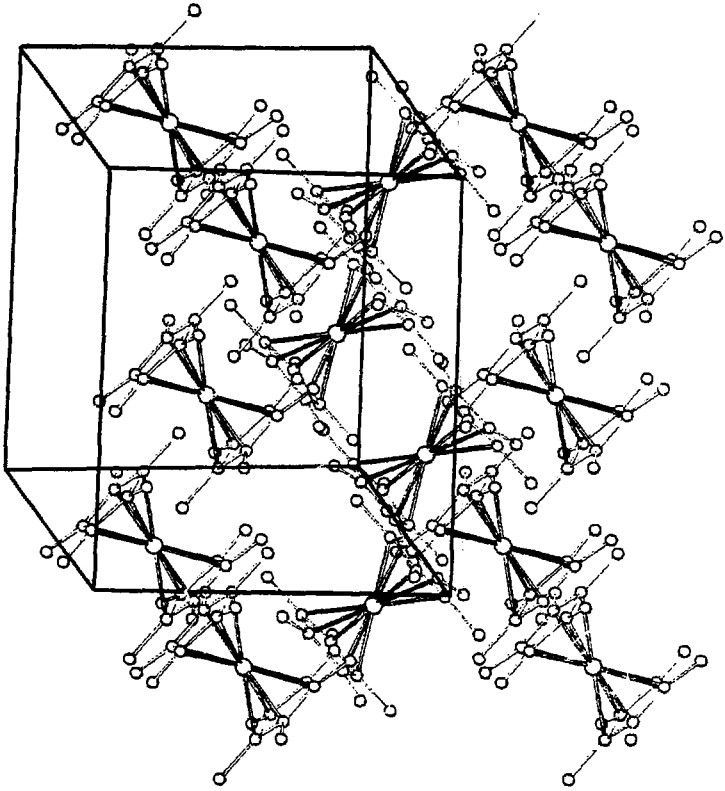

XBL 7910-12090

Figure 5. ORTEP drawing of $(Me_5Cp)_2Mn$. The nonhydrogen atoms are drawn at 50% probability contours of the thermal motion. The hydrogen atoms have an arbitrary size.

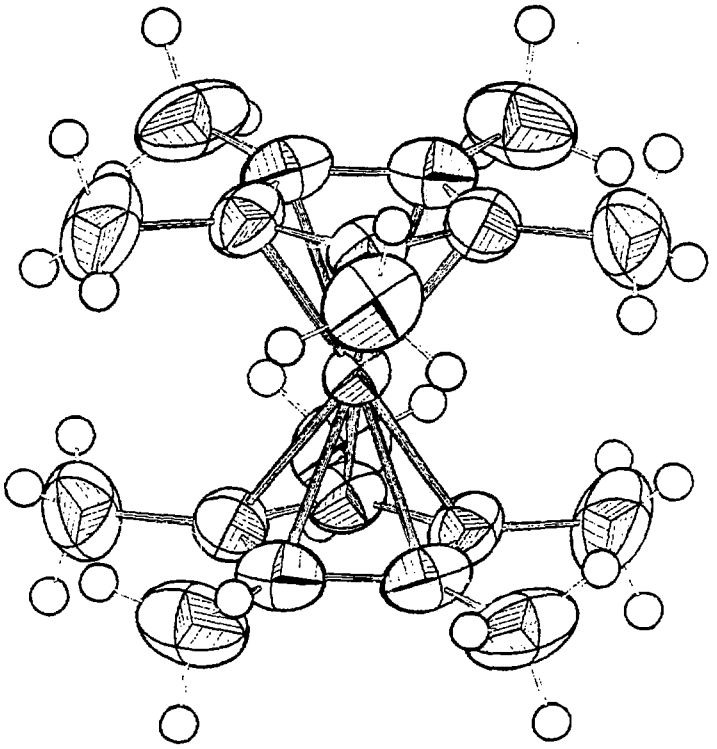

XBL 7910-12089

level plus the number of vacancies in the e_{2g} and a_{1g} levels. Thus n = 0 for Cp_2Fe, n = 1 for Cp_2Co and low-spin manganocenes, n = 2 for Cp_2Cr and Cp_2Ni, n = 3 for Cp_2V, and n = 5 for high-spin Cp_2Mn. The R(M-C)'s of these complexes, as determined by electron diffraction, are found to increase monotonically with n (Table IV).

The structures of $(Me_5Cp)_2Fe$, $[(Me_5Cp)_2Mn]PF_6$ and several other first transition series decamethylmetallocenes (whose preparation and electronic structures are described in Chapter 2) have been determined by X-ray crystallography.[47,60] All of the compounds examined (Table V) are monomeric with rings in the staggered configuration. The R(M-C)s of the cationic and neutral series of decamethylmetallocenes follow the pattern predicted by Haaland's electron imbalance model: R(M-C) increases monotonically with n. (Table V).

Summary

Magnetic studies of decamethylmanganocene show that permethylation of the Cp^- ring results in exclusively low-spin behavior, in contrast to other manganocenes where high-spin states are thermally populated. In spite of the fact that Me_5Cp^- is a much bulkier ligand than Cp^-, the metal-to-ring carbon distances in $(Me_5Cp)_2Mn$ are about 0.3 Å, shorter than those in high-spin manganocenes. This result attests to the enhanced thermodynamic stability of a manganocene with a low-spin configuration. The low-spin configuration of $(Me_5Cp)_2Mn$ also renders it inert towards ring displacement and hydrolysis, but the complex does undergo reversible oxidation and reduction to give low-spin 16- and 18-electron derivatives for which no analogs exist in other manganocenes.

Table IV. Electronic configurations, electron imbalance values, and average metal to carbon distances for first transition series metallocenes.

Compound	Electronic configuration	Electron imbalance	R(M-C)[a]	Reference
Cp_2Fe	$^1A_{1g}[e_{2g}^4 a_{1g}^2]$	0	2.064(3)	71, 74
Cp_2Co	$^2E_{1g}[e_{2g}^4 a_{1g}^2 e_{1g}^1]$	1	2.119(3)	73, 75
$(MeCp)_2Mn$	$^2E_{2g}[e_{2g}^3 a_{1g}^2]$	1	2.114(12)	72
Cp_2Cr	$^3E_{2g}[e_{2g}^3 a_{1g}^1]$	2	2.169(4)	71
Cp_2Ni	$^3A_{2g}[e_{2g}^4 e_{1g}^2]$	2	2.196(4)	76
Cp_2V	$^4A_{2g}[e_{2g}^2 a_{1g}^1]$	3	2.280(5)	77
Cp_2Mn	$^6A_{1g}[e_{2g}^2 a_{1g}^1 e_{1g}^2]$	5	2.380(5)	70
$(MeCp)_2Mn$	$^6A_{1g}[e_{2g}^2 a_{1g}^1 e_{1g}^2]$	5	2.433(8)	72

a) Distances in Å as determined by gas-phase electron diffraction.

Table V. Electronic configurations, electron imbalance values and average metal to ring carbon distances for the first transition series decamethylmetallocenes.

Compound	Electronic configuration	Electron imbalance	R(M-C)[a]	Reference
$(Me_5Cp)_2Fe$[b,d]	$^1A_{1g}[e_{2g}^4 a_{1g}^2]$	0	2.050(2)	47c
$(Me_5Cp)_2Fe$[c]	$^1A_{1g}[e_{2g}^4 a_{1g}^2]$	0	2.064(3)	78
$(Me_5Cp)_2Co$[b,d]	$^2E_{1g}[e_{2g}^4 a_{1g}^2 e_{1g}^1]$	1	2.105(3)	60
$(Me_5Cp)_2Mn$[b,e]	$^2E_{2g}[e_{2g}^3 a_{1g}^2]$	1	2.112(3)	47c
$(Me_5Cp)_2Mn$[c]	$^2E_{2g}[e_{2g}^3 a_{1g}^2]$	1	2.130(4)	47d
$[(Me_5Cp)_2Co]PF_6$[b,f]	$^1A_{1g}[e_{2g}^4 a_{1g}^2]$	0	2.049(2)	60
$[(Me_5Cp)_2Fe]PF_6$[b,f]	$^2E_{2g}[e_{2g}^3 a_{1g}^2]$	1	2.094(2)	60
$[(Me_5Cp)_2Mn]PF_6$[b,f]	$^3E_{2g}[e_{2g}^3 a_{1g}^1]$	2	2.130(2)	60
$[(Me_5Cp)_2Cr]PF_6$[b,f]	$^4A_{2g}[e_{2g}^2 a_{1g}^1]$	3	2.198(2)	60

a) Distances in Å. Values in parentheses are the average standard deviations for the 10 R(M-C) distances.

b) Determined by single crystal X-ray diffraction.

c) Determined by gas-phase electron diffraction.

d) Space group - C_{MCA}

e) Space group - $C_{2/C}$ at 298K; C_{MCA} at 100K.

f) Space group - $P_{2_1/C}$

These results indicate that the ligand field strength of the Cp^- ring is significantly enhanced by the complete replacement of the hydrogens with electron-donating methyl groups. To test this hypothesis, the decamethylmetallocenes and decamethylmetallocene cations of the other first transition series metals, V, Cr, Fe, Co, and Ni have been prepared. Magnetic susceptibility and EPR studies of these compounds establish that they are isoelectronic with their metallocene counterparts. A comparison of the UV-visible spectra of the d^3, d^6, and d^8 metallocenes and decamethylmetallocenes is used to determine the effect of complete ring alkylation on the ligand field parameters Δ_1, Δ_2, and B. These investigations are described in Chapter 2.

CHAPTER 2

Other First Transition Series Decamethylmetallocenes

EXPERIMENTAL SECTION

Preparation of Complexes

Bis(pentamethylcyclopentadienyl)Vanadium(II)

A suspension of $VCl_2 \cdot 2THF$ in THF (50 mL) was prepared from VCl_3 (3.11 g; 19.8 mmol) and Zn dust (0.65g; 9.9 mmol) using the method described by Köhler and Prössdorf.[79] The stirred suspension was added through a cannula to a solution of Me_5CpNa (4.00 g; 25.3 mmol) in THF (100 mL) and the mixture was refluxed for 7 h to yield a dark purple solution. Solvent was removed under reduced pressure and the product was heated under vacuum (60°C; 10^{-3} torr) for 6 h to remove oily contaminants. The residue was then extracted with pentane (50 mL), filtered, and washed with pentane until washings were colorless (3 x 20 mL). Solvent was again removed in vacuo to give a red, microcrystalline solid. Sublimation (100°C; 10^{-5} torr), followed by recrystallization from pentane gave $(Me_5Cp)_2V$ as air-sensitive, dark red prisms (2.60g; 65%).

Acetonitrile bis(pentamethylcyclopentadienyl)Vanadium(III) Hexafluorophosphate

Acetonitrile (40 mL) was added through a cannula to a mixture of $(Me_5Cp)_2V$ (0.20g; 0.62 mmol) and $[Cp_2Fe]PF_6$ (0.20g; 0.60 mmol). The ferricenium salt dissolved instantly with stirring yielding a deep blue solution. Over a period of 30 min., the decamethylvanadocene dissolved and reacted to give a dark green solution of the product. Solvent was removed under vacuum and the resulting solid was washed with hexane (5 x 10 mL) to remove Cp_2Fe, then dried under vacuum to

yield the crude product as an air-sensitive, dark green powder (0.22g; 96%). Olive green needles were obtained by crystallization from acetonitrile/toluene (2/1, V/V).

Dicarbonylbis(pentamethylcyclopentadienyl)Vanadium(III) Hexafluorophosphate

Carbon monoxide was passed over a stirred solution of $[(Me_5Cp)_2V(NCCH_3)]PF_6$ (0.40g; 0.79 mmol) in acetone (50 mL) for 1.5 h and the color changed from dark green to yellow. The solution was concentrated to ca. 10 mL and hexane (10 mL) was added slowly until the solution became cloudy. Upon cooling (-30°C, 12 h), the product crystallized as bright yellow prisms. The solid was filtered, washed with hexane, (2 x 10 mL) and dried under vacuum (0.38g; 78%).

Bis(pentamethylcyclopentadienyl)Chromium(II)

Solid $Cr_2(OAc)_4$ (2.15g; 6.32 mmol) was added against an argon counterstream to a solution of Me_5CpNa (4.00g; 25.28 mmol) in THF (50 mL). The mixture was stirred for 8 h at room temperature to yield a white solid suspended in a dark red solution. Decamethylchromocene was isolated from this mixture as red air-sensitive prisms (2.6g; 64%) following the procedure described above for $(Me_5Cp)_2V$.

Bis(pentamethylcyclopentadienyl)Chromium(III) Hexafluorophosphate

Tetrahydrofuran (40 mL) was added to a mixture of $(Me_5Cp)_2Cr$ (0.94g; 2.92 mmol) and $(Cp_2Fe)PF_6$ (0.92g; 2.78 mmol). The chromium compound dissolved rapidly with stirring, but the ferricenium salt dissolved only slowly. After stirring for 8 h at room temperature,

the ferricenium salt was no longer visible and the product had deposited as a yellow precipitate. This was collected by filtration then washed with THF (3 x 10 mL) and dried under vacuum to give a green-yellow solid (1.20g; 90%). Crystallization from a concentrated acetone solution yielded pure $[(Me_5Cp)_2Cr]PF_6$ as orange-yellow prisms.

Bis(pentamethylcyclopentadienyl)Cobalt(III) Hexafluorophosphate

A solution of Me_5CpH (8.00g; 58.7 mmol) in THF (200 mL) was cooled to -78°C (dry-ice/ethanol) and treated with n-butyllithium (24.5 mL; 2.4M in hexane). Upon warming to room temperature (ca. 1 h) white Me_5CpLi precipitated from a yellow solution. Solid anhydrous $CoCl_2$ (3.81g; 29.3 mmol) was added against an argon counterstream and the mixture immediately turned brown. After stirring at room temperature for 12 h, the dark brown solution was treated with solid NH_4PF_6 (5.00g; 30.7 mmol) resulting in a mildly exothermic reaction and evolution of a gas. After stirring an additional 12 h at room temperature, the mixture was filtered. The resulting brown solid was washed with THF (3 x 20 mL) then H_2O (5 x 20 mL) and dried under vacuum to give a green powder. The aqueous wash and all subsequent steps were performed in air. The green solid was extracted into acetone, filtered, and the solution concentrated to ca. 20 mL. Addition of hexane (100 mL) gave a yellow precipiate which was filtered, washed with hexane (2 x 10 mL) and dried in air to yield $[(Me_5Cp)_2Co]PF_6$ as a bright yellow air-stable powder (3.8g; 28%). Crystallization from a concentrated acetone solution gave yellow prisms.

Bis(pentamethylcyclopentadienyl)Cobalt(II)

Tetrahydrofuran (30 mL) was added to a mixture of $[(Me_5Cp)_2Co]PF_6$ (2.75g; 5.80 mmol) and Na/Hg amalgam (17.0g; .83% Na; 6.4 mmol Na). After stirring for 12 h all of the Co(III) starting material had reacted to give a clear, brown solution which was decanted from the Hg through a cannula into a Schlenk tube. Solvent was removed *in vacuo* and the product was sublimed (10^{-5} torr/100°C) then crystallized from hexane to yield $(Me_5Cp)_2Co$ as dark brown, air-sensitive prisms (1.60g; 84%).

Bis(pentamethylcyclopentadienyl) Nickel(II)

Pentamethylcyclopentadiene (8.00g; 58.7 mmol) in THF (350 mL) was deprotonated with n-butyllithium (25.0 mL; 2.37 M in hexane) at -78°C as described in the preparation of $[(Me_5Cp)_2Co]PF_6$. Solid $NiBr_2 \cdot 2DME$ (9.06g; 29.4 mmol) was added against an argon counterstream to the Me_5CpLi suspension at room temperature and the mixture was stirred for one dat at room temperature to yield a dark brown solution. Following the procedure described in the isolation of $(Me_5Cp)_2V$, $(Me_5Cp)_2Ni$ was obtained as dark green prisms (5.5g; 57%). Several sublimations were required to separate the product from a yellow, pentane soluble, but involatile impurity.

Bis(pentamethylcyclopentadienyl) Nickel(III) Hexafluorophosphate

Decamethylnickelocene (1.40g; 4.25 mmol) and $(Cp_2Fe)PF_6$ (1.30g; 3.93 mmol) were allowed to react in THF in the manner described above in the preparation of $[(Me_5Cp)_2Cr]PF_6$ to give $[(Me_5Cp)_2Ni]PF_6$ as a brown powder (1.67g; 90%). Crystallization from acetone afforded dark brown prisms. The BF_4^- salt was prepared similarly from

$[Cp_2Fe]BF_4$ and $(Me_5Cp)_2Ni$.

Bis(pentamethylcyclopentadienyl)Nickel(IV) bis(Hexafluorophosphate)

Tetrahydrofuran (30 mL) was added to a mixture of solid $(Me_5Cp)_2Ni$ (0.83g; 2.52 mmol) and solid $HgCl_2$ (0.68g; 2.51 mmol). The solids dissolved rapidly and an orange precipitate separated from a pale green solution. The mixture was stirred for 1 h then filtered. The orange precipitate was washed with THF (2 x 10 mL) and dried under vacuum. Subsequent reactions were performed in air. The product (1.46g) was dissolved in 0.1 M aqueous HCl (10 mL) to give an orange solution and a metallic precipitate. The solution was filtered then treated with solid NH_4PF_6 (1.5g). A yellow-brown solid immediately precipitated. This was filtered, then extracted with warm (40°C) 0.1 M aqueous HCl (10 x 30 mL). The solvent volume was reduced under vacuum to ca. 10 ml and the product crystallized as orange prisms which were collected on a fritted disc filter, washed with cold H_2O, (2 x 5 ml) and dried in air (0.60g; 38%). Recrystallization from warm 0.1 M HCl gave an analytically pure sample.

Solid $[(Me_5Cp)_2Ni](PF_6)_2$ decomposes slowly (over a period of a week) in air, under vacuum, or under an argon atmosphere to a paramagnetic dark brown material. The complex decomposes instantly in $(CH_3)_2CO$ or CH_3CN solution, but is stable for several days in acidic aqueous solution. The PF_6^- salt was not sufficiently soluble in aqueous solution to allow determination of the ring carbon chemical shift in the ^{13}C NMR spectrum although the methyl carbon atom resonance was observed at δ 9 ppm after 26,000 pulses. To determine

the complete ^{13}C NMR spectrum, a sample of the orange precipitate from the $HgCl_2/(Me_5Cp)_2Ni$ reaction (0.3g) was dissolved in a minimum volume of 0.1 M HCl (1 mL), filtered, treated with a deficiency (~ 50%) of NH_4PF_6 to precipitate $[(Me_5Cp)_2Ni]PF_6$ and any paramagnetic impurities, then filtered again. The resulting solution was diamagnetic, as determined by the Evans NMR method.[59] The optical spectrum of a diluted aliquot of this solution was identical to that of the pure PF_6^- salt. The concentrated solution of $[(Me_5Cp)_2Ni]Cl_2$ was then transferred to a coaxial NMR tube with C_6D_6 in the inner capillary to provide a deuterium lock and reference for the ^{13}C chemical shifts.

Bis(pentamethylcyclopentadienyl)Magnesium(II)

A solution of i-PrMgCl in THF (66 mL; 1.2 M; 79.2 mmol) was transferred with a syringe into a flask containing Me_5CpH (10.0g; 73.4 mmol). Toluene (125 mL) was added through a cannula and the mixture was stirred at 80°C for 6 h to give an orange solution. 1,4-Dioxane (70 mL) was added and a small quantity of a white solid, $MgCl_2 \cdot$1,4-dioxane, precipitated. The mixture was stirred at 80°C for 36 h. During this time additional white solid precipitated. The solution was cooled to room temperature, filtered, and the resulting white solid washed with toluene (2 x 20 mL). The solution was reduced under vacuum to an orange oil which was freed of volatile liquids by evacuation overnight at 70°C. The flask was then fitted with a water cooled probe and $(Me_5Cp)_2Mg$ was sublimed (90°C; 10^{-5} torr) as a white, crystalline, air-sensitive solid (4.45g; 41%). Resublimation gave an analytically pure sample. The product

crystallizes from hexane as colorless prisms. Analytical, mass spectral, and infrared data for these compounds are given in Table VI.

RESULTS AND DISCUSSION

Synthesis and Characterization

The syntheses of the decamethylmetallocenes frequently requires modifications of the commonly used routes to the metallocenes and the 1,1'-dimethylmetallocenes. For example, the reaction $MCl_3 + 3\ Na^+RCp^- \rightarrow (RCp)_2M + RCp\cdot + 3\ NaCl$ (R = H or Me) has been used in the preparation of vanadocenes and chromocenes [43] where one equivalent of cyclopentadienide serves to reduce the trivalent metal salts. However, the hydrocarbon soluble products derived from the reaction of three equivalents of Me_5CpNa with VCl_3 or $CrCl_3$ in THF are intractable oils containing only small amounts of the desired products. The isolation of pure decamethylmetallocenes from these reaction mixtures is complicated by the presence of the pentamethylcyclopentadiene dimer, [80] a colorless solid whose volatility and solubility properties are quite similar to those of the desired products. These results suggest that efficient routes to neutral decamethylmetallocenes require the use of divalent metal starting materials.

Köhler and Prössdorf [79] have reported the preparation of $(RCp)_2V$ (R = H or Me) from the reaction of $VCl_2\cdot 2THF$, with two equivalents of Na^+RCp^- in THF. We find that $(Me_5Cp)_2V$ may also be prepared by this route. Me_5CpLi may be substituted for Me_5CpNa, but a significant reduction in yield results. We have also obtained

Table VI. Physical, analytical, and infrared data for decamethylmetallocenes.

Compound	Melting point	Mass spectrum[a] (P+)	Infrared[b] (cm^{-1})	Analysis calcd. (fd.)
$(Me_5Cp)_2V$	299-300°C	321(100)	587(w), 463(m), 422(w), 233(w)	C, 74.74(74.90); H, 9.41(9.15)
$[(Me_5Cp)_2V(NCCH_3)]PF_6$	-	-	459(m), 442(w), ν_{CN} = 2270(s)	C, 52.07(52.24); H, 6.55(6.31) N, 2.76(2.75); P, 6.11(5.93)
$[(Me_5Cp)_2V(CO)_2]PF_6$	-	-	515(m), 454(w) ν_{CO} = 1989(s), 1954(s), 1975(w), 1902(w)	C, 50.58(50.69); H, 5.79(5.84) P, 5.93(5.79)
$(Me_5Cp)_2Cr$	296-297°C	322(100)	585(m), 418(m), 235(w)	C, 74.49(74.34); H, 9.09(9.09)
$[(Me_5Cp)_2Cr]PF_6$	-	-	525(m), 440(w), 412(w)	C, 51.39(51.50); H, 6.47(6.39) P, 6.63(6.63)
$(Me_5Cp)_2Co$	294-296°C	329(100)	586(m), 429(w), 320(w), 232(w)	C, 72.93(73.06); H, 9.18(9.11)
$[(Me_5Cp)_2Co]PF_6$	-	-	590(w), 448(m), 362(m), 255(w)	C, 50.54(50.79); H, 6.37(6.35) P, 6.53(6.42)
$(Me_5Cp)_2Ni$	296-297°C	328(100)	587(w), 385(m), 320(w)	C, 72.98(73.03); H, 9.19(9.07)
$[(Me_5Cp)_2Ni]PF_6$	-	-	472(w), 225(w)	C, 50.66(50.41); H, 6.38(6.27) P, 6.53(6.68)
$[(Me_5Cp)_2Ni](PF_6)_2$	-	-	468(w), 432(m), 328(m), 248(m)	C, 38.80(38.63); H, 4.88(4.88) P, 10.01(9.81)
$(Me_5Cp)_2Mg$	289-292	294(308)	587(w), 560(m), 517(s), 427(m), 283(m), 210(w)	C, 81.49(82.65); H, 10.26(10.15)

a) 70 eV. Only parent ion reported. m/e (relative abundance).

b) Absorptions between 600 and 200 cm^{-1} reported. Between 4000 and 600 cm^{-1} infrared spectra are superimposable with characteristic absorptions at 2989(m), 2940(m), 2895(s), 2850(m), 2750(w), 1470(m), 1448(m), 1422(m), 1373(m), 1355(w), 1065(m), 1023(w), 722(w) cm^{-1}. The PF_6^- salts also show bands at 874(s), 845(s), 725(m), 552(m), 530(m) cm^{-1}.

nearly quantitative yields of $(Me_5Cp)_2V$ from the reaction of Me_5CpNa with VCl_2 (pyridine)$_4$ in THF.[81]

Köhler and Prössdorf also describe the synthesis of $(RCp)_2Cr$ from the reaction of a cyclopentadienide with $CrCl_2 \cdot THF$.[79] We find that readily available $Cr_2(OAc)_4$ reacts with four equivalents of $(Me_5Cp)Na$ in THF to afford $(Me_5Cp)_2Cr$ in good yield. Again, Me_5CpLi may be substituted, but with reduction of yield.

The modest yield obtained in the synthesis of $[(Me_5Cp)_2Co]PF_6$ merits some comments. Both Cp_2Co and $(MeCp)_2Co$ are obtained in high yields from the reaction of the cyclopentadienide with $CoCl_2$.[43,82] in THF, but anhydrous cobaltous salts (e.g., $CoCl_2$, $CoBr_2$, and $Co(OAc)_2$) react with Me_5Cp^- (as the Li^+, Na^+, or Mg^{2+} salts) in THF to give a complex mixture of products, most of which are insoluble in non-polar solvents.[83] Isolation of pure $(Me_5Cp)_2Co$ from the crude reaction mixture is complicated by the presence of other volatile hydrocarbon soluble products, but oxidation of the reaction mixture with NH_4PF_6 affords the air-stable $[(Me_5Cp)_2Co]PF_6$ as a yellow precipitate in 28% yield. Subsequent reduction of the cation with Na/Hg in THF gives $(Me_5Cp)_2Co$ in high yield. Decamethylnickelocene is prepared <u>via</u> the reaction of $NiBr_2 \cdot 2DME$ with two equivalents of Me_5CpLi in THF. Koelle and Khouzami have recently reported that $(Me_5Cp)_2Co$ and $(Me_5Cp)_2Ni$ are obtained in 80 to 90% yield from the reaction of $MBr_2 \cdot 1,2$-dimethoxyethane (M = Co or Ni) with $(Me_5Cp)Li$ in a refluxing <u>mixture</u> of THF and diethyl ether.[35] Although these would appear to be the preferred routes to the nickel and cobalt compounds, the authors do not state the THF/diethyl ether ratio required to achieve such high yields. The disproportionation of

$(Me_5Cp)MgCl$ with 1,4-dioxane in toluene solution affords $(Me_5Cp)_2Mg$. Elemental carbon analyses for $(Me_5Cp)_2Mg$ proved consistently high. This may be due to its extreme air sensitivity.

The neutral decamethylmetallocenes are very soluble in aromatic and aliphatic hydrocarbon solvents as well as THF, diethyl ether, and dichloromethane, but are only slightly (ca. 10^{-3} M) soluble in acetone or acetonitrile.[86] They melt in the range 290 to 300°C and are volatile, subliming at temperatures greater than 70°C (10^{-5} torr). The neutral compounds are air-sensitive in solution. In THF solution, $(Me_5Cp)_2Mg$ is instantly hydrolyzed by water and reacts with $FeCl_2$ to give $(Me_5Cp)_2Fe$. In THF, the V, Cr, and Co compounds are oxidized to their cationic derivatives by water. The neutral Ni and Fe compounds are unaffected by water. The neutral V, Cr, Co, and Ni compounds react with $FeCl_2$ in THF to yield cationic decamethylmetallocenes but no detectable amounts of $(Me_5Cp)_2Fe$. The Cp_2M compounds of V, Cr, Fe and nickel do not react with water in THF, but Cp_2Co is oxidized to Cp_2Co^+. Reactions of Cp_2Cr or Cp_2V with $FeCl_2$ yielded Cp_2Fe.[43] Cobaltocene is oxidized to Cp_2Co^+ and Cp_2Ni is unaffected by $FeCl_2$ in THF.[43]

Like the first transition series metallocenes, the permethylated compounds undergo facile one-electron oxidation to isolable monocationic derivatives. The $[(Me_5Cp)_2M]PF_6$ salts (M = Cr, Mn, Co, Ni) are obtained in nearly quantitative yield *via* the reaction of $(Me_5Cp)_2M$ with one molar equivalent of $(Cp_2Fe)PF_6$ in THF. Decamethylcobaltocene and decamethylchromocene are very strong reducing agents (see Table VII): both are oxidized by proton sources such as H_2O and NH_4^+. In contrast, Cp_2Cr^+ has been prepared only by oxidation

of Cp_2Cr with allyl iodide[87] or carbon tetrachloride.[88] The reaction of chromocene with $(Cp_2Fe)PF_6$ results in extensive decomposition.[46b]

The $[(Me_5Cp)_2M]PF_6$ compounds are very soluble in acetone, acetonitrile, and dichloromethane, sparingly soluble in THF and diethyl ether, and insoluble in aromatic and aliphatic hydrocarbon solvents. The cationic Fe, Co, and Ni compounds are air stable solids. The Cr(III) complex decomposes very slowly in air. This result is surprising since the $[Cp_2Cr]I$ is reported to be very air sensitive.[87] The cationic Cr, Mn, and Ni compounds are air sensitive in solution.

The cyclic voltammograms of $[(Me_5Cp)_2Cr]PF_6$ (Figure 6), $[(Me_5Cp)_2Co]PF_6$ (Figure 7), and $[(Me_5Cp)_2Ni]PF_6$ (Figure 8) in dry, oxygen-free acetonitrile show that each complex is reduced in a reversible step with a peak separation close to 59 mV, the theoretical value for a reversible one-electron process.[56] The reduction potentials of the decamethylmetallocene cations are as much as 500 mV more negative than those of the unsubstituted compounds (Table VII). Along similar lines, a UV-PES study of the $(Me_5Cp)_2M$ compounds in the gas-phase showed that both ligand- and metal-ionizations are about 1 eV lower in energy in the peralkylated derivatives than the corresponding ionizations of the Cp_2M compounds.[63] The enhanced stability of the decamethylmetallocene cations is attributed to the electron-donating properties of the substituent methyl groups.

The cyclic voltammogram of $[(Me_5Cp)_2Ni]PF_6$ (Figure 8) consists of two reversible one-electron steps at -0.65 and +0.31 V vs. SCE. Since $(Me_5Cp)_2Ni$ is unaffected by strong reducing agents such as

Figure 6. Cyclic voltammogram of $[(Me_5Cp)_2Cr]PF_6$ in CH_3CN on Pt disc electrode with 0.1 M $[(n\text{-butyl})_4N]BF_4$ electrolyte. Scan rate = 100 mV sec^{-1}.

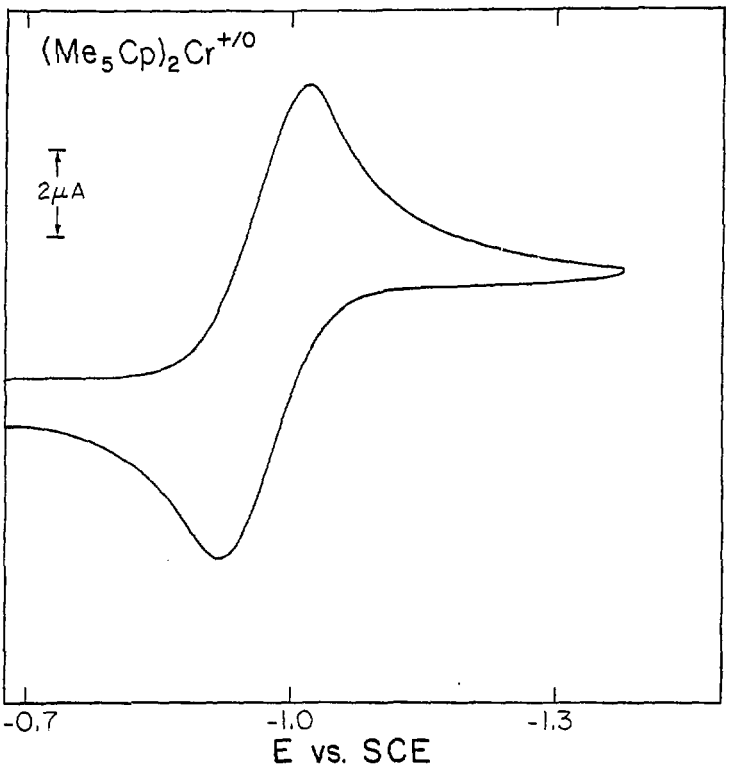

XBL 797-2325

Figure 7. Cyclic voltammogram of $[(Me_5Cp)_2Co]PF_6$ in CH_3CN on Pt disc electrode with 0.1 M $[(n\text{-butyl})_4N]BF_4$ electrolyte. Scan rate = 100 mV sec^{-1}.

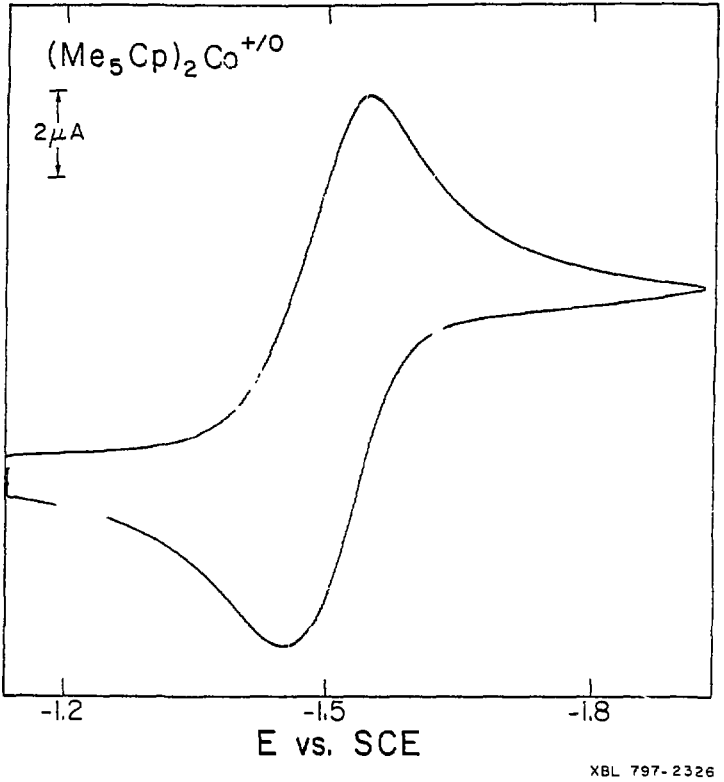

XBL 797-2326

Figure 8. Cyclic voltammogram of $[(Me_5Cp)_2Ni]PF_6$ in CH_3CN on Pt disc electrode with 0.1 M $[(n\text{-butyl})_4N]BF_4$ electrolyte. Scan rate = 100 mV sec^{-1}.

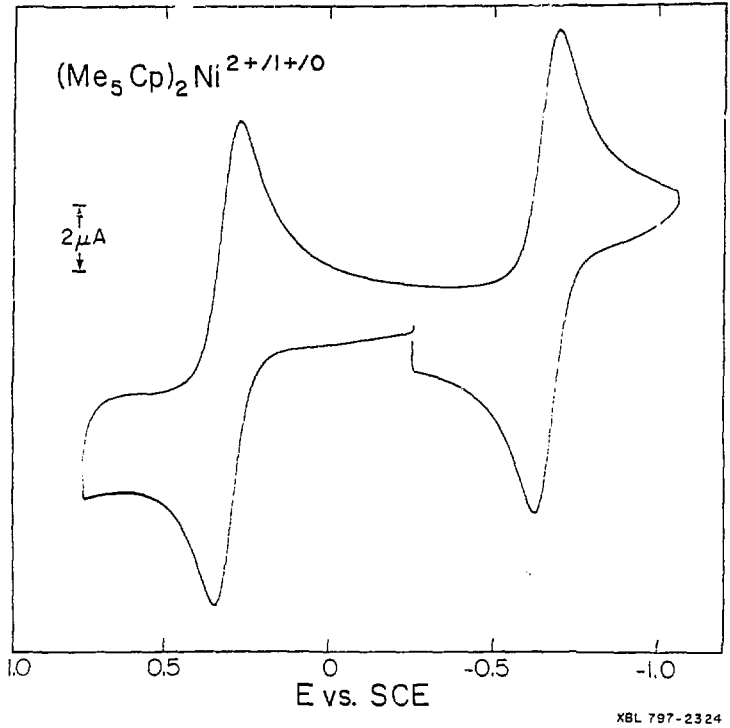

XBL 797-2324

Table VII. Metallocene and Decamethylmetallocene electrochemical data.

Metallocenes	$E_{1/2}$ [a]	Reference	Decamethylmetallocenes	$E_{1/2}$ [a,b]	Reference
$(Cp_2Cr)^+$	-0.55[c]	89	$[(Me_5Cp)_2Cr]^+$	-1.04	This work
$(Cp_2Fe)^+$	+0.41	This work	$[(Me_5Cp)_2Fe]^+$	-0.12	This work, 85
$(Cp_2Co)^+$	-0.91	58a	$[(Me_5Cp)_2Co]^+$	-1.47	This work
$(Cp_2Ni)^+$	-0.09	90, 91	$[(Me_5Cp)_2Ni]^+$	-0.65	This work
$(Cp_2Ni)^{2+}$	+0.77	90, 91	$[(Me_5Cp)_2Ni]^{2+}$	+0.31	This work

a) Half wave potentials for the reaction $[(R\text{-}Cp)_2M]^{n+} + e^- \rightleftarrows [(R\text{-}Cp)_2M]^{(n-1)+}$ given in volts with reference to the saturated calomel electrode.

b) Determined by cyclic voltammetry in CH_3CN solution with 0.1 M $[(n\text{-butyl})_4N]BF_4$ electrolyte.

c) The reversibility of this wave in CH_3CN solution is questionable, reference 89.

Na/Hg or sodium naphthalide, these potenials must correspond to the $(Me_5Cp)_2Ni^+/(Me_5Cp)_2Ni$ and $(Me_5Cp)_2Ni^{2+}/(Me_5Cp)_2Ni^+$ redox couples. Formally, this may be viewed as a Ni(II), Ni(III), Ni(IV) system analogous to the $[(B_9C_2H_{11})_2Ni]^{2-/1-/0}$ complexes isolated by Hawthorne, et al.[90] Van Duyne[91] and Hawthorne[90] have independently reported electrochemical evidence for the existence of $(Cp_2Ni)^{2+}$ in dry acetonitrile, but to date there has been no report of either its isolation or characterization in solution.

In acetone or acetonitrile solution $[(Me_5Cp)_2Ni]PF_6$ reacts with Ce(IV), O_2, Ag^+, or H_2O_2 to give an amorphous, green, paramagnetic solid. However, treatment of a THF solution of $(Me_5Cp)_2Ni$ with one molar equivalent of $HgCl_2$ results in immediate precipitation of an orange solid. This dissolves in 0.1 M aqueous HCl to yield colloidal Hg and a solution of $[(Me_5Cp)_2Ni]^{2+}$, which was subsequently isolated as the crystalline, orange-brown PF_6^- salt. The infrared spectrum of $[(Me_5Cp)_2Ni](PF_6)_2$ in the range 4000 to 700 cm^{-1} is similar to the spectra of the $[(Me_5Cp)_2M]PF_6$ compounds (see below). An Evans' NMR method measurement[59] shows that the complex is diamagnetic in solution. We conclude that $[(Me_5Cp)_2Ni]^{2+}$ is a planar, 18-electron decamethylmetallocene, isoelectronic with $[(Me_5Cp)_2Mn]^-$, $(Me_5Cp)_2Fe$, and $[(Me_5Cp)_2Co]^+$.

The decamethylnickelocene dication is a metastable complex. The solid PF_6^- salt slowly decomposes to a brown solid, even in the absence of air. In cold, acidic, aqueous solution the complex is stable for several days, but in neutral or basic solution it is rapidly reduced to the Ni(III) derivative. Dissolution of the dication in acetonitrile or acetone, or addition of these solvents to an aqueous solution of the

complex, results in decomposition to the same green substance obtained in attempts to oxidize $(Me_5Cp)_2Ni^+$ in nonaqueous solvents.

The cyclic voltammogram of $(Me_5Cp)_2V$ in acetonitrile solution is complex and exhibits no reversible one-electron waves. Decamethylvanadocene is rapidly oxidized by $(Cp_2Fe)PF_6$ in THF, but the blue product polymerizes the solvent. In acetone, acetonitrile, or diethyl ether solution, $(Me_5Cp)_2V$ reacts with $(Cp_2Fe)PF_6$ to yield paramagnetic, solvated V(III) complexes corresponding to the formulation $[(Me_5Cp)_2VS]PF_6$ (S = solvent). Attempts to remove the solvent from these compounds by heating under vacuum resulted in decomposition. This behavior parallels that of $(Cp_2V)^+$, which is also isolated as a solvated species in the absence of a coordinating anion (such as Cl^- or Br^-),[92,93] and further demonstrates the coordinative unsaturation of metallocenes with a 14-electron configuration.[10] Like $(Cp_2V)^+$, the permethylated derivative reacts with CO (1 atm) to give the diamagnetic 18-electron dicarbonyl complex, $[(Me_5Cp)_2V(CO)_2]PF_6$.[94] As King has found in a comparison of cyclopentadienyl- and pentamethylcyclopentadienyl metal carbonyls, the CO stretching frequencies occur at substantially lower energy in the permethylated compound (νCO = 1990, 1936 cm^{-1}) than in the unsubstituted derivative (νCO = 2050, 2010 cm^{-1}).[95] We follow King in suggesting that this effect is due to the influence of electron-donating methyl groups which increase electron density on the metal center, thereby enhancing the M-CO, and weakening the C-O bonds.[45]

The D_{5d} metallocene structure has been established by X-ray crystallography for $(Me_5Cp)_2M$ (M = Mn, Fe, Co) and $[(Me_5Cp)_2M]PF_6$ (M = Cr, Mn, Fe, Co).[47c, 60] Infrared spectra of the neutral

transition metal compounds are superimposible in the range 4000 to 600 cm^{-1} with characteristic absorptions found between 2800 and 3000 cm^{-1} (4 bands), 1350 and 1500 cm^{-1} (5 bands), and 1000 and 1100 cm^{-1} (2 bands). Infrared spectra of the cationic complexes are similar but more poorly resolved. Since these bands are insensitive to changes in metal ion, oxidation state, and even geometry (e.g., the "bent" $[(Me_5Cp)_2V(CO)_2]^{++}$ and $[(Me_5Cp)_2V(solvent)]^{+}$ complexes, they must represent primarily ligand vibrational modes for the π-bound Me_5Cp^- ligand. Below 600 cm^{-1}, where metal-ring vibrations are expected to occur, the infrared spectra vary from compound to compound. Specific infrared data in this region are listed in Table VI.

A comparison of the ^1H and ^{13}C NMR data for diamagnetic Me_5Cp^- compounds (Table VIII) shows that the chemical shift of the ring carbon atom is very sensitive to the electronic effects induced by variation of the metal ion. For the planar transition metal compounds, the order of decreasing chemical shift, $\delta(Ni) > \delta(Co) > \delta(Fe) > \delta(Mn)$, follows the expected order of increasing metal to ring electron donation.

Magnetic Susceptibility and EPR

15 and 20-electron systems.

The magnetic properties of the metallocenes have been thoroughly investigated, both from an experimental and a theoretical viewpoint.[35,65,66] The simplest behavior is found for systems with orbitally nondegenerate ground states, that is compounds with 15-electron $^4A_{1g}$ (Cp_2V and Cp_2Cr^+) or 20-electron, $^3A_{2g}$ (Cp_2Ni) configurations. No orbital contributions to the moment are expected and furthermore, species with

Table VIII. ^{1}H and ^{13}C NMR data for diagmagnetic Me_5Cp^- compounds.[a]

Compound	^{1}H	^{13}C[b]		solvent
		ring C	methyl C	
Me_5CpNa	2.01	105.1	11.8	THF-d_8
$(Me_5Cp)_2Mg$	1.93	110.1	9.6	C_6D_6
$[(Me_5Cp)_2V(CO)_2]PF_6$	2.00	107.4	9.3	$(CD_3)_2CO$
$Na[(Me_5Cp)_2Mn]$	1.83	72.4	8.5	THF-d_8
$(Me_5Cp)_2Fe$	1.70	78.4	9.6	C_6D_6
$[(Me_5Cp)_2Co]PF_6$	1.78	93.4	6.3	$(CD_3)_2CO$
$[(Me_5Cp)_2Ni]^{2+}$	2.20	118.3[c]	9.4[c]	D_2O

a) All values in parts per million (δ) vs. tetramethylsilane.

b) Proton decoupled.

c) Values determined for the Cl^- salt in 0.1 M aqueous HCl.

these configurations are not subject to Jahn-Teller distortions which can alter magnetic parameters (vide infra). Consequently, magnetic moments close to the spin-only value are expected. Magnetic susceptibility measurements on vanadocenes and nickelocenes have confirmed these expectations. The complexes obey the Curie-Weiss law ($\chi_m = C/(T-\theta)$) over a wide temperature range and moments within experimental error of the spin-only values (2.87 μ_B for S = 1; 3.89 μ_B for S = 3/2)[66] are found (Table IX).

Prins and co-workers observed that the Cp_2Ni magnetic susceptibility curve deviates from Curie-Weiss behavior below 70K, and the susceptibility becomes essentially independent of temperature below 30K.[100] They found that this result could be attributed to the influence of a large zero field splitting on an otherwise nondegenerate triplet ground state. The magnitude of the zero field splitting (25.6 cm^{-1}) was taken as conclusive evidence that the two unpaired electrons reside in a molecular orbital which is substantially metal rather than ligand in character, indicating a $^3A_{2g}$ $[e_{2g}^4 a_{1g}^2 e_{1g}^2]$ or $^3A_{2u}$ $[e_{2g}^4 a_{1g}^2 e_{1u}^2]$ ground state formulation. The former ground state has been assigned on the basis of UV-visible[41] and UV-PES[42b] studies of Cp_2Ni. The existence of a large zero field splitting explains why no EPR signal is observed for Cp_2Ni.[101,102]

The χ_m^{-1} vs. T curve for $(Me_5Cp)_2Ni$ (Figure 9) is very similar to that determined for Cp_2Ni by Prins, et al. (see Figure 1 of reference 100). Above 20K, the curve is linear, yielding an effective moment (2.93 ± 0.1 μ_B) close to the spin-only value for an S = 1 molecule. A similar moment is observed in solution at room temperature (Table IX). Below 25K, the curve flattens and χ_m^{-1} becomes virtually

Table IX. Magnetic susceptibility data for metallocenes and decamethylmetallocenes.

	Solid			Solution		
Compound	μ_{eff}[b]	θ	temp. range[c]	μ_{eff}[b]	temp.[c]	Reference
$(Me_5Cp)_2V$	3.69±0.1	0	5-64	3.78±0.1	304	This work
Cp_2V	3.78±0.2	6.5	14-430	3.78	298	96,98
$[(Me_5Cp)_2Cr]PF_6$	3.73±0.1	0	4.5-81	3.74±0.1	304	This work
$(Cp_2Cr)I$	3.87		90-296	-	-	87
$(Me_5Cp)_2Cr$	3.01±0.1	0	6-81	2.90±0.1	304	This work
Cp_2Cr	3.20±0.16	17	90-295	3.10	298	97,98
$(Me_5Cp)_2Co$	1.45±0.1	0	5-130	1.56±0.1	304	This work
Cp_2Co	1.75±2.04[d]		83-298	1.76	298	66,98
$[(Me_5Cp)_2Ni]PF_6$	1.67±0.1[f]	28	5-75	1.44±0.1	304	This work
$[(Me_5Cp)_2Ni]BF_4$	1.62±0.1	0	6-57	-	-	This work
$(Cp_2Ni)B(C_6H_5)_4$	1.82±0.15		90-300	-	-	99
$(Me_5Cp)_2Ni$	2.93±0.1[e]	-15	6-100	2.89±0.1	304	This work
Cp_2Ni	2.89±0.15[e]	6	70-300	2.86	298	98,100

a) Measured in toluene or acetonitrile solution by the Evans NMR method.[59]

b) Values in Bohr Magnetons.

c) Temperatures in degrees K.

d) θ value uncertain because of curvature in χ_m^{-1} vs. T plot.

e) Moments and θ-values obtained from the linear portion of the χ_m^{-1} vs. T curve.

f) Antiferromagnetic. Nee'l temperature = 18K.

Figure 9. $1/\chi_m$ (mole/emu) vs. T plot for crystalline $(Me_5Cp)_2Ni$.

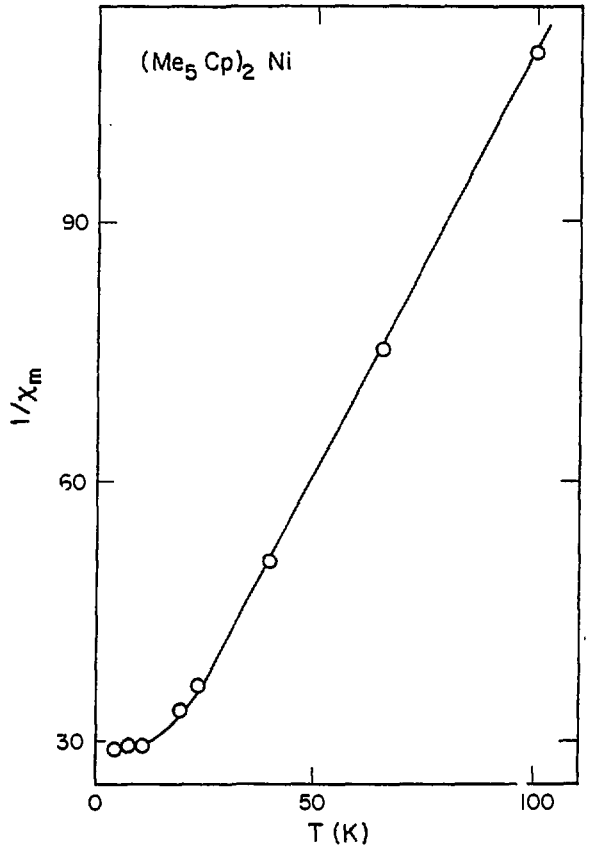

XBL 798-2692

independent of temperature. Magnetization data throughout the temperature range display a normal, linear magnetic field dependence, so ferromagnetism may be ruled out as an explanation for the unusual magnetic behavior observed at low temperatures.

As was found for Cp_2Ni, the $(Me_5Cp)_2Ni$ magnetic susceptibility data can be accounted for using a model which considers the influence of a large zero field splitting on a nondegenerate, triplet ground state. According to Prins, et al. the molar susceptibility at high-temperature (i.e., in the linear range of the χ_m^{-1} T curve) is given by equation 1, and at low temperature

$$\chi_m = \frac{2}{9} \frac{N\mu_B^2}{kT} (g_{||} + 2g_{\perp}^2) \qquad (1)$$

$$\chi_m = \frac{4}{3} N\mu_B^2 \frac{g_{\perp}^2}{D} \qquad (2)$$

by equation 2 where N is Avogadro's number, μ_B is the Bohr Magneton, k is the Boltzmann constant, T is the temperature, and D is the zero field splitting parameter in cm^{-1}.[100] Following Prins, the free electron value (2.0023) is assumed for $g_{||}$. Experimental data then yield $g_{\perp} = 1.74$ from equation 1 and $D = 30.5 \pm 1.0\ cm^{-1}$ from equation 2. The D- and μ_{eff}-values found for $(Me_5Cp)_2Ni$ are close to those obtained for Cp_2Ni, so these compounds appear have the same electronic ground state. No EPR signal is observed for $(Me_5Cp)_2Ni$ in toluene solution either at 10K or 298K, presumably because of the magnitude of the zero field splitting parameter.

Magnetic susceptibility and EPR studies of the 15-electron metallocenes Cp_2V and $(Cp_2Cr)^+$ indicate that they possess an orbitally

nondegenerate $^4A_{2g}$ $[e_{2g}^2\ a_{1g}^{\perp}]$ ground state. The magnetic moments of Cp_2V and $(Cp_2Cr)I$ are close to the spin-only value for an S = 3/2 system and are independent of temperature (Table IX). The EPR spectra of Cp_2V and $(Cp_2Cr)^+$ diluted in diamagnetic hosts consist of resonance near g = 2 ($g_{||}$; $m_s = -3/2 \rightarrow m_s = -1/2$) and g = 4 ($g_{\perp}$; $m_s = -3/2 \rightarrow m_s = +1/2$) (Table X). Vanadocene EPR spectra exhibit ^{51}V (I=7/2) hyperfine coupling on both resonances at low temperature.[41,68,103] Ammeter has shown that the g- and A-values for Cp_2V are essentially independent of the host matrix employed.[68] This situation is to be contrasted with that found for metallocenes with orbitally degenerate ground states (e.g., cobaltocene and low-spin manganocenes) whose EPR spectra show a pronounced host dependence.[68]

Bulk magnetic susceptibility measurements on $(Me_5Cp)_2V$ and $[(Me_5Cp)_2Cr]PF_6$ show simple Curie behavior ($\chi_m = C/T$) in the temperature range 5 to 70K. The magnetic moments obtained from these measurements are in agreement with the solution values at room temperature (Table IX) and are close to the spin-only value for S = 3/2 molecules. These data imply a $^4A_{2g}$ ground state, an assignment that is confirmed by EPR spectroscopy.

The EPR spectra of $(Me_5Cp)_2V$ and $[(Me_5Cp)_2Cr]^+$ (Figures 10-13) diluted in diamagnetic host lattices exhibit resonances near g = 2 and g = 4 (Table X) and are quite similar to the spectra reported for Cp_2V and $(Cp_2Cr)^+$. Signals are observed both at room- and liquid helium temperature , although the room temperature spectra are somewhat broadened. The g- and A-values are insensitive to changes in host matrix, a result that is in accord with a nondegenerate configuration. Metal hyperfine coupling is resolved only on $g_{\perp}$ for the Cr derivative

Table X. EPR data for 15-electron metallocenes and decamethylmetallocenes.

Compound	Host	Temp.[a]	$g_{\parallel}$	$g_{\perp}$[b]	$A_{\parallel}$[c]	$A_{\perp}$[c]	Reference
$(Me_5Cp)_2V$	toluene	19	2.001(1)	3.973(1)	24.0(0.2)	16.0(0.2)	This work
	toluene	300	$\langle g \rangle$ = 1.985		$\langle A \rangle$ = 23.1(0.2)		This work
	$(Me_5Cp)_2Mg$	24	2.005(2)	3.991(1)	23.2(0.2)	17.1(0.2)	This work
Cp_2V	methylcyclohexane	77	1.990(2)	4.004(1)	36.7(1.0)	21.5(0.5)	41
	2-methyltetrahydrofuran	4	1.9888(4)	4.0040(6)	36.3(0.2)	20.9(0.2)	68
	Cp_2Mg	4	1.9882(4)	4.0028(6)	36.3(0.2)	20.9(0.2)	68
$[(Me_5Cp)_2Cr]PF_6$	$[(Me_5Cp)_2Co]PF_6$	9	2.001(1)	4.02(1)	d	253(2)	This work
	$[(Me_5Cp)_2Co]PF_6$	300	2.004(1)	4.03(2)	d	d	This work
$[(Me_5Cp)_2Cr]^+$	$(Me_5Cp)_2Mg$[e]	17	1.99(1)	4.01(1)	d	d	This work
$(Cp_2Cr)^+$	Cp_2Mg[e]	4	2.002(2)	3.954(2)	d	d	68

a) Temperatures in degrees K.

b) This is a "half-field" resonance corresponding to a $\Delta m_s = 2$ transition. The true $g_{\perp}$ values are one half of those reported.

c) In units of 10^{-4} cm^{-1}.

d) Hyperfine coupling not resolved.

e) Spectra of the neutral chromocenes cosublimed with Cp_2Mg or $(Me_5Cp)_2Mg$.

Figure 10. X-band EPR spectrum of $(Me_5Cp)_2V$ diluted in toluene at 19K.

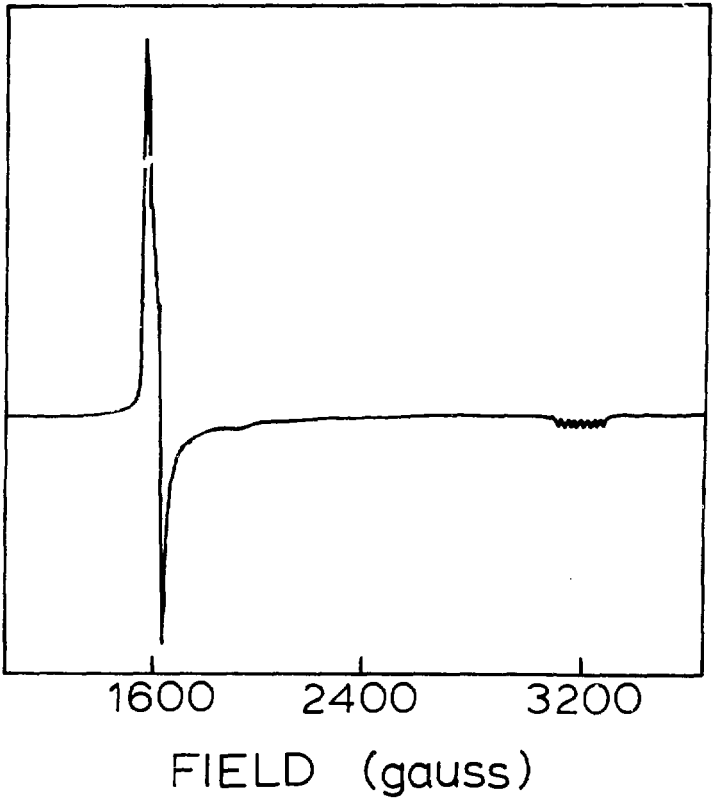
1600
2400
3200
FIELD (gauss)

Figure 11. X-band EPR spectrum of $(Me_5Cp)_2V$ diluted in toluene at 19K. Expansion of the g = 2.001 resonance.

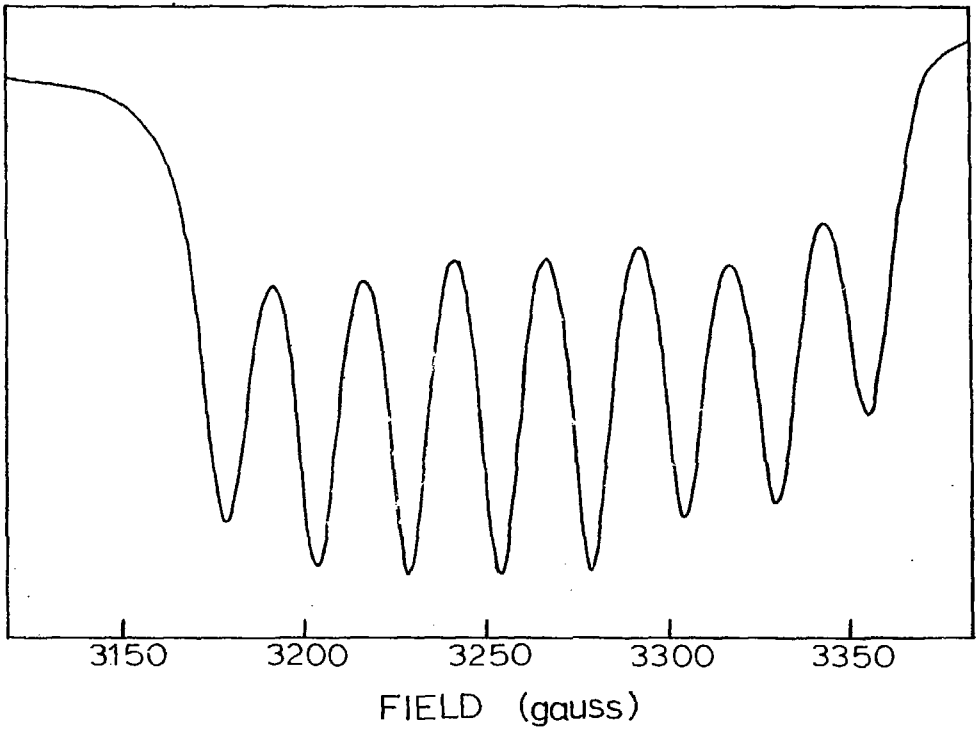
3150
3200
3250
3300
3350
FIELD (gauss)

Figure 12. X-band EPR spectrum of $(Me_5Cp)_2V$ diluted in toluene at 19K. Expansion of the g = 3.973 resonance.

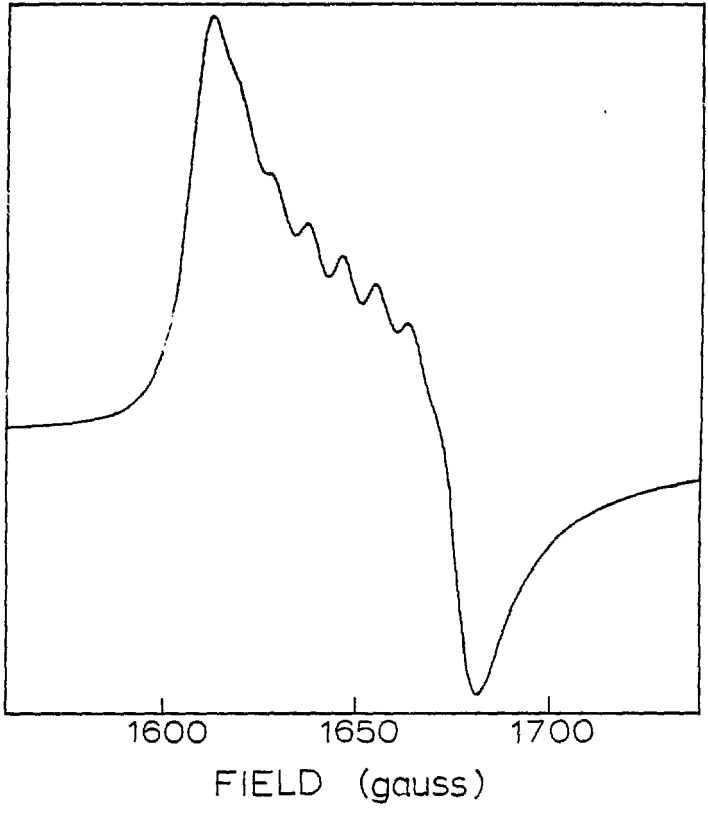
1600
1650
1700
FIELD (gauss)

Figure 13. X-band EPR spectrum of $[(Me_5Cp)_2Cr]PF_6$ diluted in $[(Me_5Cp)_2Co]PF_6$ at 9K.

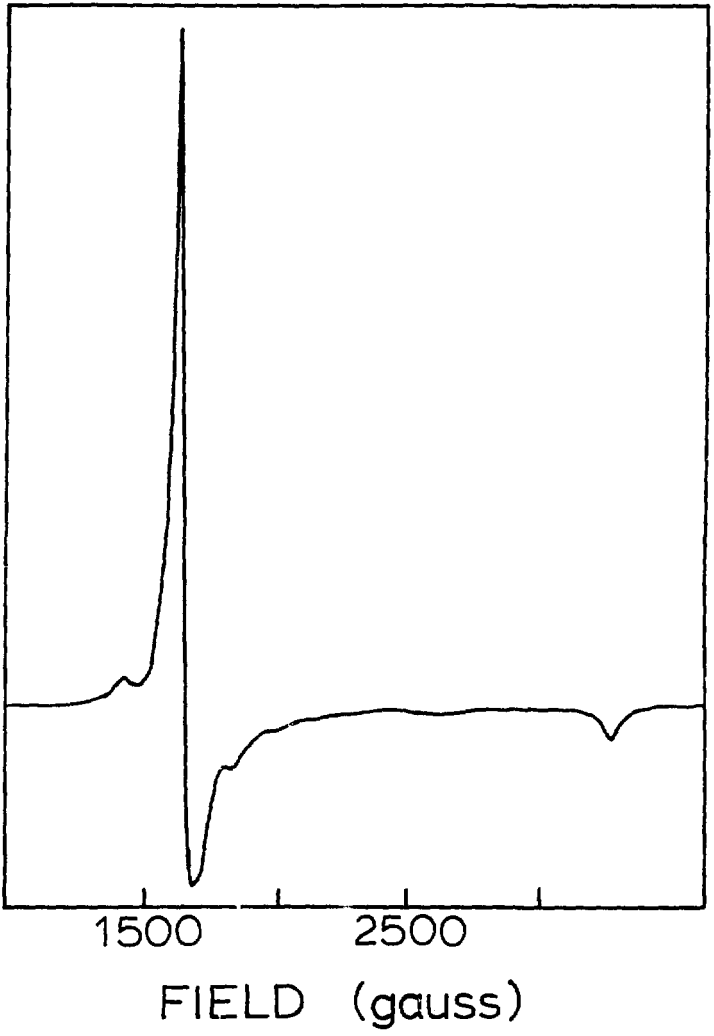
1500
2500
FIELD (gauss)

(^{53}Cr, I = 3/2, 9.55% natural abundance), but is found on both $g_{\perp}$ and $g_{||}$ for the vanadium compound (^{51}V, I = 7/2, 99% natural abundance).

Prins and Van Voorst have derived expressions that allow determination of the metal orbital mixing coefficients C_o^2 (metal 4s), C_δ^2 (metal e_{2g}), and C_σ^2 (metal a_{1g}) for $^4A_{2g}$ metallocenes from the g- and A-values (see equation 2 of reference 41). Using these expressions (with a minor modification suggested by Ammeter[104]) we have calculated these parameters for Cp_2V and $(Me_5Cp)_2V$. In both cases, the most reasonable (i.e., positive) sets of parameters are obtained with the assumption of negative values for the hyperfine coupling constants. A comparison of the C_o^2, C_σ^2, and C_δ^2 values for vanadocene and decamethylvanadocene (Table XI) shows that C_o^2 and C_σ^2 are essentially the same in both compounds. However, C_δ^2 is substantially smaller in the peralkylated derivative, indicating increased delocalization of the metal e_{2g} electrons over the ligand π-orbitals. Since the ligand e_{2g} level is antibonding (with respect to the rings) and unoccupied in the free ligand, this result implies that Me_5Cp^- can act as a stronger π-acid than Cp^- and the covalency of the metal-ring bond is enhanced by complete alkylation of the ring.

16- and 19-Electron Complexes

Magnetic susceptibility,[65,66] EPR,[35] and UV-photoelectron[42b] studies have established that the 16-, low-spin 17-, and 19-electron metallocenes possess orbitally degenerate $^3E_{2g}$ [$e_{2g}^3\ a_{1g}^1$], $^2E_{2g}$ [$e_{2g}^3\ a_{1g}^2$], and $^2E_{1g}$ [$e_{2g}^4\ a_{1g}^2\ e_{1g}^1$] electronic configurations,

Table XI. Metal orbital mixing coefficients for vanadocene and decamethylvanadocene.

	C_o^2	C_π^2	C_δ^2
Cp_2V[a]	0.22	0.78	0.65
$(Me_5Cp)_2V$[b]	0.25	0.75	0.53

a) Calculated from EPR data in reference 41.

b) Calculated from $(Me_5Cp)_2V$ in toluene (19K) EPR spectrum.

respectively. The theoretical expectations for the magnetic parameters of such systems prove to be more complex than the relatively simple treatment applied to metallocenes with non-degenerate ground states. For example, significant orbital contributions to the magnetic moment are expected, an effect which would in general produce temperature dependent moments that are greater than the spin-only value.[65] Warren's ligand field calculations indicate that increased delocalization of the unpaired (metal) electron over ligand π-orbitals (a decrease of the orbital reduction factor, k') will serve to reduce the moments towards the spin-only value.[65] The systems under consideration are also subject to Jahn-Teller distortions from pure axial symmetry. Warren calculates that a large static C_{2v} distortion of these metallocenes will result in temperature independent moments that are close to the spin-only value.[65]

These theoretical considerations indicate that magnetic moments of orbitally degenerate metallocenes may be expected to lie within a rather large range of values (see tables A through F of reference 65). Although this result appears to be somewhat ambiguous, it has proven useful in the assignment of a ground state of metallocenes for which either an orbitally degenerate or nondegenerate electronic configuration is possible. Thus, for low-spin 17-electron metallocenes the observation of moments that are significantly greater than the spin-only value for S = 1/2 was taken as evidence for the orbitally degenerate $^2E_{2g}$ configuration rather than the nondegenerate $^2A_{1g}$ ground state (see Chapter 1).

Two low-spin ground states are also possible for 16-electron metallocenes: the orbitally degenerate $^3E_{2g}$ $[e_{2g}^3\ a_{1g}^1]$ configuration and the nondegenerate $^3A_{2g}$ $[e_{2g}^2\ a_{1g}^2]$ configuration. Magnetic susceptibility studies of Cp_2Cr and $(MeCp)_2Cr$ gave moments (ca. 3.2 μ_B; Table IX) substantially larger than the spin-only value for S=1 systems (2.87 μ_B) indicating a $^3E_{2g}$ ground state assignment.[66] This assignment has also been proposed from a UV-PES study of the chromocenes.[42b]

In Chapter 1, it was noted that solid $[(Me_5Cp)_2Mn]PF_6$ obeys the Curie-Weiss law with an effective moment of 3.07 ± 0.1 μ_B. Bulk susceptibility measurements on $(Me_5Cp)_2Cr$ indicate simple Curie behavior with μ_{eff} = 3.01 ± 0.1 μ_B up to 80K. The solid state and solution magnetic susceptibility data for both complexes (Tables II and IX) are consistent with a triplet ground state, but the magnetic moments are only slightly greater than the spin-only value, so the choice between $^3A_{2g}$ and $^3E_{2g}$ ground state assignments is ambiguous. However, a recent UV-photoelectron study of $(Me_5Cp)_2Cr$ and $[(Me_5Cp)_2Mn]^+$ has established that these complexes possess an orbitally degenerate $^3E_{2g}$ ground state in the gas-phase.[63]

Like Cp_2Cr, $(Me_5Cp)_2Cr$ and $[(Me_5Cp)_2Mn]^+$ are EPR silent. No signal was observed for the neutral chromium compound in toluene solution (10K or 298K). Samples of $(Me_5Cp)_2Cr$ cosublimed with $(Me_5Cp)_2Mg$ do give strong EPR signals at liquid helium and room temperature, but these are due to the fortuitous presence of the oxidized derivative, $[(Me_5Cp)_2Cr]^+$ (see Table X).

Magnetic susceptibility measurements on the 17-electron metallocenes Cp_2Co and $(Cp_2Ni)^+$ have shown that they are low-spin

complexes with one unpaired electron (Table IX). The most recent measurements on Cp_2Co revealed that the moment is temperature dependent in the range 83 to 298K, in accord with an orbitally degenerate ground state (vide supra).[66] EPR studies of Cp_2Co and $(Cp_2Ni)^+$ indicate that the unpaired electron resides in a molecular orbital that is substantially metal in character, so the $^2E_{1g}$ $[e_{2g}^4 a_{1g}^2 e_{1g}^1]$ ground state has been assigned.

The effects of static and dynamic Jahn-Teller distortions have proven important in the interpretation of the EPR spectra of the 19-electron, $^2E_{1g}$ metallocenes.[68,105-108] Under pure axial symmetry, the g-values are given by $g_{||} = 2(k'+1)$, $g_{\perp} = 0$ (k' is the orbital reduction factor) and no $g_{\perp}$ signal is expected.[65] A theoretical treatment which considered the effect of a static C_{2v} distortion predicted the g-values according to equations 3 and 4 where c and

$$g_{||} = g_z = 2-4k'cs \tag{3}$$

$$g_{\perp} = g_x = g_y = 2(c^2-s^2) \tag{4}$$

s are coefficients of the lowest Kramer's doublet: $\phi^{\pm} = c\phi_4^{\pm} \pm s\phi_5^{\pm}$ (ϕ_4 and ϕ_5 are the wavefunctions of the $2e_{1g}$ orbital).[106] Neither of these results proved satisfactory as the EPR spectra of Cp_2Co and $(Cp_2Ni)^+$ diluted in diamagnetic hosts consist of <u>three</u> resonance-near g = 2 (Table XII), clearly indicating that $g_{\perp}$ is anisotropic ($g_x \neq g_y$).[68,106] Ammeter and Swalen demonstrated that the anisotropy of $g_{\perp}$ could result from <u>dynamic</u> Jahn-Teller coupling.[106] This effect is a consequence of the breakdown of the Born-Oppenheimer

Table XII. EPR data for 19-electron metallocenes and decamethylmetallocenes.

Compound	Host	Temp.[a]	g_x	g_y	g_z	A_x[b]	A_y[b]	A_z[b]	Reference
	toluene	14		g_{iso}=2.0		-	-	-	This work
$(Me_5Cp)_2Co$	methyl-cyclohexane	15		g_{iso}=1.8		-	-	-	This work
	$(Me_5Cp)_2Fe$[c]	9	1.693(3)	1.733(8)	1.754(1)	< 6	111(3)	65(1)	This work
	2-methyl THF	4	$g_{\perp}$=1.81		1.69	-	-	-	68
Cp_2Co	Cp_2Fe	4	1.755	1.847(3)	1.693(2)	-	-135	-85.6	108
	Cp_2Mg	4	1.637	1.627	1.638(3)	-92.8	-111	-94.6	108
$[(Me_5Cp)_2Ni]PF_6$	$[(Me_5Cp)_2Co]PF_6$	8	1.973(1)	2.014(1)	1.831(2)	-	-	-	This work
	$(Cp_2Co)PF_6$	4	1.972(1)	2.015(1)	1.800(8)	-	-	-	68,108
$(Cp_2Ni)^+$	$(Cp_2Co)BF_4$	4	1.865(1)	1.915(1)	1.744(2)	-	-	-	68,108
	$(Cp_2Co)SbF_6$	4	1.642(5)	1.692(8)	1.700(8)	-	-	-	68,108

a) Temperatures in degrees K.

b) In units of 10^{-4} cm^{-1}.

c) Calculated from Figure 11. Includes second order shift. Signs for A-values uncertain.

approximation due to vibronic coupling of degenerate or near-degenerate electronic states. In this treatment, the g- and A-tensors are found to be a function of the orbital reduction factor (k'), a vibronic reduction factor (V), and α, a measure of the static distortion from five-fold symmetry.[106] Ammeter and co-workers have subsequently demonstrated that the g-tensors of Cp_2Co and $(Cp_2Ni)^+$ (and A-tensor of Cp_2Co) are very sensitive to alkyl substitution of the Cp^- ring and to variation of the diamagnetic host matrix. Their analysis indicates that dynamic Jahn-Teller distortions predominate over static distortions, but are gradually suppressed (relative to the static distortions) by increasing asymmetry of the guest molecule and/or host lattice.[68,108]

Solid $(Me_5Cp)_2Co$ obeys the Curie Law in the temperature range 6-130K. The solid state and solution magnetic data (Table IX) yield a moment (ca. 1.5 μ_B) that is significantly smaller than the spin-only value for an S = 1/2 system (1.73 μ_B). The χ_m^{-1} vs. T curve for $[(Me_5Cp)_2Ni]PF_6$ (Figure 14) reveals a pronounced departure from simple Curie-Weiss behavior and is suggestive of antiferromagnetic coupling. Above 30K, the curve is linear, yielding an effective moment of 1.67 μ_B. χ_m^{-1} has a minimum at about 18K, then it monotonically increases with decreasing temperature to 4.2K. In contrast, the χ_m^{-1} vs. T plot for the BF_4^- salt of $[(Me_5Cp)_2Ni]^+$ (Figure 14) follows the Curie Law and yields a moment (1.62 μ_B) that is strikingly close to that obtained from the linear range of the $[(Me_5Cp)_2Ni]PF_6$ χ_m^{-1} vs. T plot. This result substantiates the contention that the unusual magnetic behavior of the PF_6^- salt has intermolecular rather than intramolecular origins.

Figure 14. $1/\chi_m$ (mole/emu) vs. T plot for solid $[(Me_5Cp)_2Ni]PF_6$ and $[(Me_5Cp)_2Ni]BF_4$.

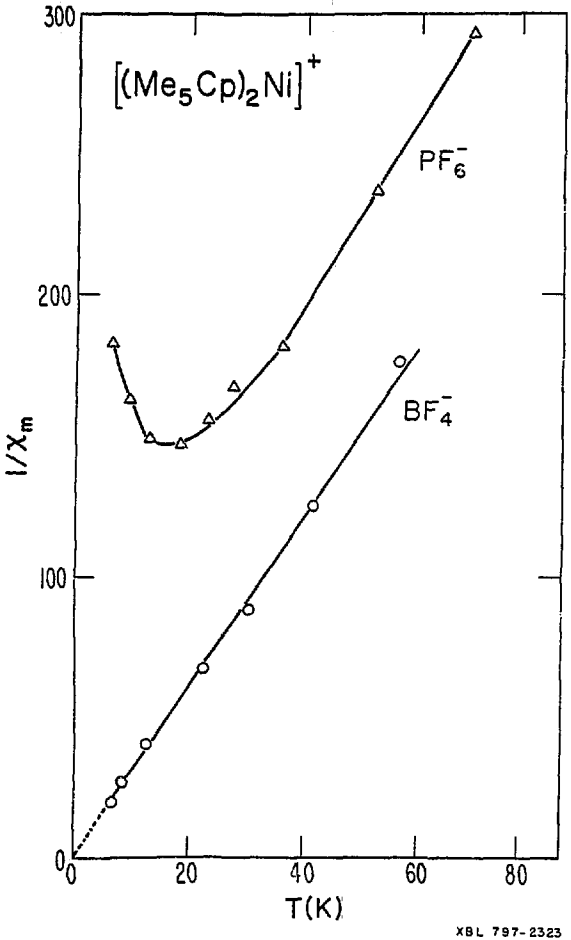

XBL 797-2323

The EPR spectra of $(Me_5Cp)_2Co$ and $[(Me_5Cp)_2Ni]^+$ are consistent with a $^2E_{1g}$ ground state. At 9K, the spectrum of $[(Me_5Cp)_2Ni]PF_6$ diluted in $[(Me_5Cp)_2Co]PF_6$ (Figure 15) exhibits three resonances near g=2 (Table XII). The g-values are close to those reported for $(Cp_2Ni)^+$ diluted in $(Cp_2Co)^+$ matrices and the spectrum is nearly identical to that of $(Cp_2Ni)PF_6$ diluted in $(Cp_2Co)PF_6$, (see Figure 17 of reference 68). No EPR signal is observed for $(Cp_2Ni)^+$ or $[(Me_5Cp)_2Ni]^+$ at room temperature. This result is not surprising since molecules with orbitally degenerate ground states typically possess very short relaxation times.

The EPR spectrum of $(Me_5Cp)_2Co$ was measured in several diamagnetic hosts. In toluene or methylcyclohexane glasses at 6K, the spectrum exhibits a broad resonance centered near g=2 and spread over a range of ca. 1200 gauss, with superimposed ^{59}Co (I=7/2) hyperfine coupling. The number of lines observed (> 10) requires that the g-tensor be anisotropic, but the spectra are not sufficiently well resolved to allow determination of the g- and A-values. Much better resolution is obtained in the EPR spectrum of $(Me_5Cp)_2Co$ diluted in $(Me_5Cp)_2Fe$. The spectrum and its assignment are shown in Figure 16. Our axis assignment of the g- and A-tensors is tentative, but follows the general observation that $A_y > A_z > A_x$ for cobaltocenes. No EPR signal is observed for $(Me_5Cp)_2Co$ in any of these environments at room temperature. EPR data for $(Me_5Cp)_2Co$ and Cp_2Co in diamagnetic hosts are compared in Table XII. It is apparent that the g- and A-values at both compounds are extremely sensitive to changes in the host matrix, but in general the EPR parameters of Cp_2Co and $(Me_5Cp)_2Co$ in matrices of

similar composition appear to be comparable.

The observation of an EPR signal for $(Me_5Cp)_2Co$ and $[(Me_5Cp)_2Ni]^+$ is evidence that the compounds are distorted from pure axial symmetry. The sensitivity of the $(Me_5Cp)_2Co$ EPR spectrum to changes in the host lattice reflects the influence of molecular environment on the nature and magnitude of the distortions. In diamagnetic decamethylmetallocene hosts both complexes exhibit anisotropic g-tensors ($g_x \neq g_y \neq g_z$). According to the arguments of Ammeter, this is a consequence of Jahn-Teller distortions that are dynamic in nature. In this context, it is noteworthy that the single crystal X-ray diffraction study of $(Me_5Cp)_2Co$ provides evidence for a static distortion from D_{5d} symmetry at room temperature.[60] The observed distortion is very similar to that reported for $(Me_5Cp)_2Mn$[47c] involving variation of ring carbon-ring carbon distances from 1.412(1) to 1.434(1) Å. In the $(Me_5Cp)_2Fe$ structure, these distances remain constant at 1.419(1) Å. Root mean square vibrational amplitudes for ring carbon atoms in the Mn, Fe, and Co compounds are comparable and this would seem to argue against the dynamic Jahn-Teller motion implied by the EPR investigation. However, it has been suggested that subtle dynamic motion in these systems is masked by the magnitude of the thermal motion at room temperature. Low temperature crystallographic studies are planned to test this notion. More detailed single crystal EPR studies of these compounds diluted in an array of diamagnetic hosts are now underway in another laboratory.[111] These investigations should provide a more quantitative assessment of the relative importance of dynamic and static Jahn-Teller distortions in the orbitally degenerate decamethylmetallocenes.

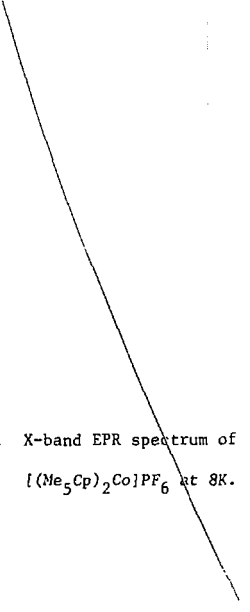

Figure 15. X-band EPR spectrum of $[(Me_5Cp)_2Ni]PF_6$ diluted in $[(Me_5Cp)_2Co]PF_6$ at 8K.

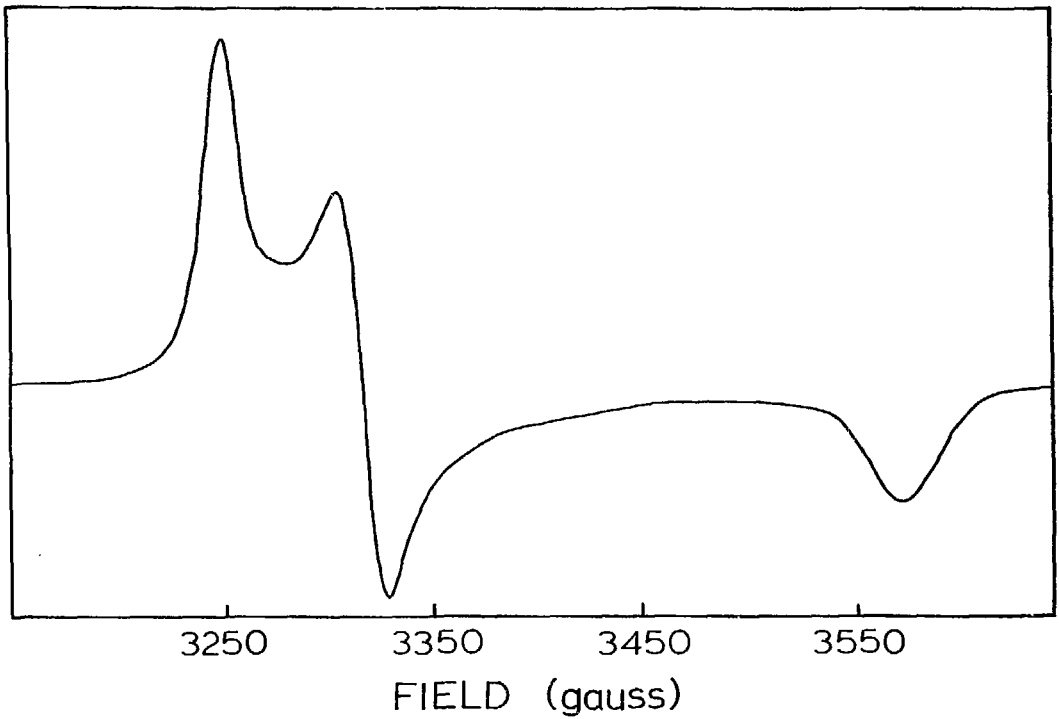
3250
3350
3450
3550
FIELD (gauss)

Figure 16. X-band EPR spectrum of $(Me_5Cp)_2Co$ diluted in $(Me_5Cp)_2Fe$ at 9K with g- and A-tensors indicated.

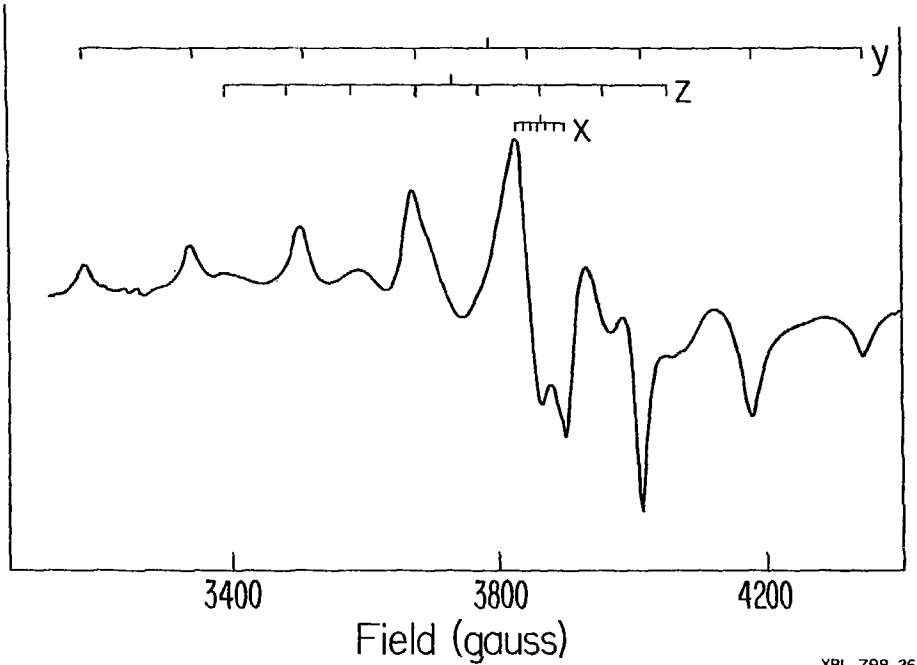

XBL 798-2696

Electronic Spectra

Having determined the ground electronic configurations of the decamethylmetallocenes, we turn now to an examination of their excited electronic states by a UV-visible spectroscopy. We pay particular attention to the ligand field (d-d) transitions since a complete assignment of the ligand field spectrum can yield the 3d-orbital splitting parameters, (Δ_1 and Δ_2) and the Racah electron repulsion parameters, B and C. This result is gemane to our purposes since in Chapter 1 we ascribed the low spin nature of $(Me_5Cp)_2Mn$ (viz a viz the high spin complexes Cp_2Mn and $(MeCp)_2Mn$) to a substantial increase in the ligand field strength of the Cp^- ring upon permethylation. Such an effect should be apparent from a comparison of the ligand field parameters of isoelectronic metallocenes and decamethylmetallocenes. Furthermore, quantitative comparisons are possible.

Using a strong field approach, ligand field theory predicts three spin-allowed d-d transitions for metallocenes with an 18-electron, $^1A_{1g}$ ground state.[40] The one-electron transition $2a_{1g} \rightarrow 2e_{1g}$ gives rise to a single excited state of $^1E_{1g}$ symmetry. The one-electron transition $1e_{2g} \rightarrow 2e_{1g}$ yields two excited states of $^1E_{1g}$ and $^1E_{2g}$ symmetries. In order to differentiate between the two $^1E_{1g}$ states, we denote the former as $^1E_{1g}(a)$ and the latter, $^1E_{1g}(b)$. Three spin-forbidden transitions (singlet $\rightarrow$ triplet) are also predicted. These excited states have the same symmetry labels as the corresponding spin-allowed states, with the exception of the spin multiplicity. Sohn, et al. have given the transition energy expressions (including configuration interaction) for the spin-allowed and spin-forbidden d-d transitions (Table I of reference

40). With the energies of the three relatively weak (singlet) absorption bands observed in the optical spectra of Cp_2Fe, Cp_2Ru, and $[Cp_2Co]^+$, they used these expressions to calculate Δ_1, Δ_2 and B with the assumption C = 4.0B (Table VIII).

The expectations for 15-electron ($^4A_{2g}$) and 20-electron ($^3A_{2g}$) metallocenes are similar. The one-electron transitions from the $2a_{1g}$ and $1e_{2g}$ levels to the $2e_{1g}$ level yield three spin-allowed excited states of $E_{1g}(a)$, E_{2g}, and $E_{1g}(b)$ symmetry.[41] Prins and Van Voorst[41] found three relatively weak absorption bands in the optical spectra of Cp_2V and Cp_2Ni. In accordance with a ligand field assignment, these bands decreased in relative intensity and shifted to higher energy at low temperature. With consideration of configuration interaction between the $E_{1g}(a)$ and $E_{1g}(b)$ states, the authors derived transition energy expressions for the excited ligand field states and calculated Δ_1, Δ_2, and B from the spectral data (Tables XIV, XV). As Sohn and co-workers found for 18-electron metallocenes, only one ligand field assignment scheme, $E_{1g}(b) > E_{2g} > E_{1g}(a)$, yielded physically reasonable (non-imaginary) B-values. A re-examination of the Cp_2V and Cp_2Ni absorption spectra by Pavlik, Cerny, and Maxova[109,110] revealed additional very weak absorptions ($\varepsilon < 1$) that were assigned to spin-forbidden d-d transitions.[35]

Warren and Gordon have demonstrated that the $^3E_{2g}$, $^2E_{2g}$, and $^2E_{1g}$ electronic configurations determined for low-spin 16-, 17-, and 19-electron metallocenes give rise to a large number of spin-allowed ligand field excited states.[66] Ligand field bands observed in the spectra of Cp_2Cr, $[Cp_2Fe]^+$, and Cp_2Co were poorly resolved and an unambiguous assignment was not possible.[35,40,66] Ligand field spectra of the analogous $(Me_5Cp)_2M$ (M = Cr, Mn, Co) and

$[(Me_5Cp)_2M]^+$ (M = Mn, Fe, Ni) complexes are also rather featureless, and they will not be discussed here.

The shoulders found at 23.8, 29.5, and 40.0 kK (1 kK = 10^3 cm^{-1}) in the spectrum of $[(Me_5Cp)_2Co]PF_6$ (Figure 17) are assigned to the three spin-allowed ligand field transitions, $^1A_{1g} \rightarrow {}^1E_{1g}(a)$, $^1E_{2g}$, $^1E_{1g}(b)$. Spectra of concentrated solutions or thick single crystals of $[(Me_5Cp)_2Co]PF_6$ reveal three very weak absorptions at 12.7, 18.5 and 21.3 kK (Figure 18) which we assign to the three spin-forbidden ligand field transitions. A weak, but sharp, peak is observed at 8.4 kK. This band could not be rationalized in terms of a ligand field assignment, so we suggest that it is due to a vibrational overtone.

The spectrum of $(Me_5Cp)_2Fe$ (Figure 19) exhibits only two bands (23.5, 30.5 kK) whose intensity suggests a ligand field assignment. The two shoulders at 34.5 and 36.0 kK neither shift to lower energy nor decrease in intensity at 77 K (methylcyclohexane glass) so a charge transfer assignment is indicated. Nonetheless, both shoulders are rather broad and fairly intense, so it is reasonable to propose that the third ligand field band is hidden in this region. We therefore use 34.5 kK as a <u>minimum</u> estimate for the energy of the $^1A_{1g} \rightarrow {}^1E_{2g}(b)$ transition in the calculation of ligand field parameters for $(Me_5Cp)_2Fe$.

The spectrum of $[(Me_5Cp)_2Ni]^{2+}$ (Figure 20) consists of a weak absorption at 22.5 kK, intense peaks at 31.5 and 40.9 kK, and a shoulder at <u>ca</u>. 42.5 kK. The 22.5 kK band is assigned to the $^1A_{1g} \rightarrow {}^1E_{1g}(a)$ transition. <u>If</u> the shoulder at 42.5 kK is due to the highest energy ligand field state ($^1E_{1g}(b)$), then the intermediate $^1E_{2g}$ excited state must be masked by one of the intense charge transfer

Figure 17. Electronic spectrum of $[(Me_5Cp)_2Co]PF_6$ in acetonitrile solution.

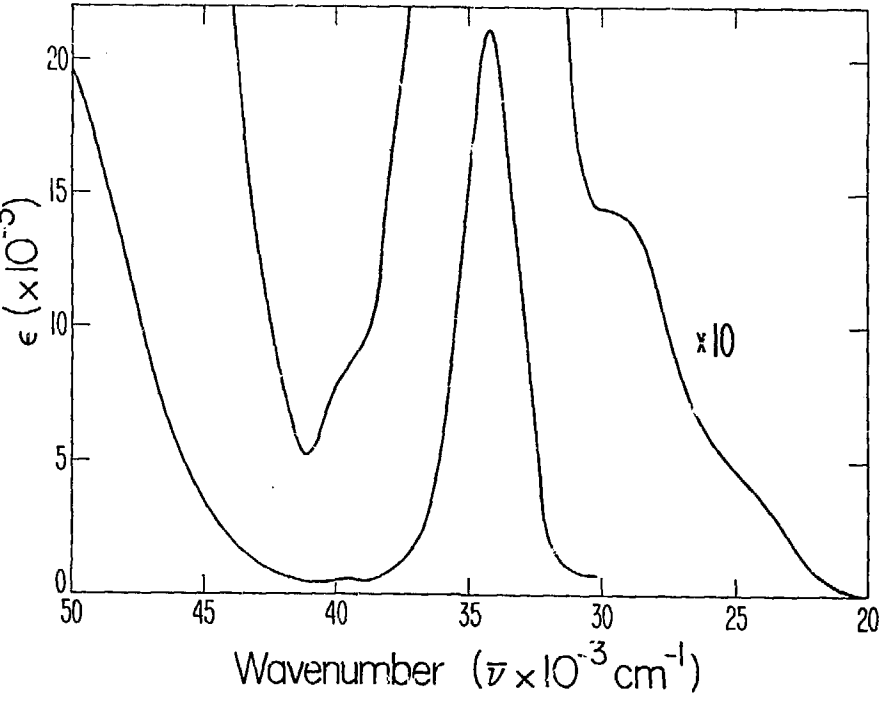
20
15
10
5
0
ϵ ($\times 10^{-3}$)
50
45
40
35
30
25
20
Wavenumber ($\bar{\nu} \times 10^{-3}$ cm^{-1})
x10

XBL 796-2695

Figure 18. Electronic spectrum of a concentrated acetonitrile solution of $[(Me_5Cp)_2Co]PF_6$ and a thin single crystal of $[(Me_5Cp)_2Co]PF_6$. The molar absorptivity (ε) scale applies only to the solution spectrum. The intensity scale for the single crystal spectrum is arbitrary absorbance units.

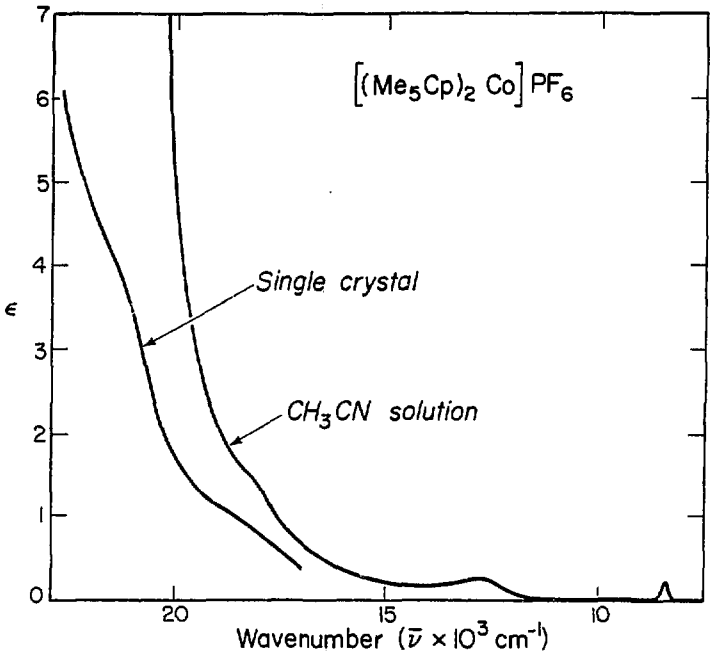
[(Me5Cp)2 Co] PF6
Single crystal
CH3CN solution
ε
0
1
2
3
4
5
6
7
20
15
10
Wavenumber (ν̄ × 10³ cm⁻¹)

XBL 799-2923

Figure 19. Electronic spectrum of $(Me_5Cp)_2Fe$ in methylcyclohexane solution at room temperature.

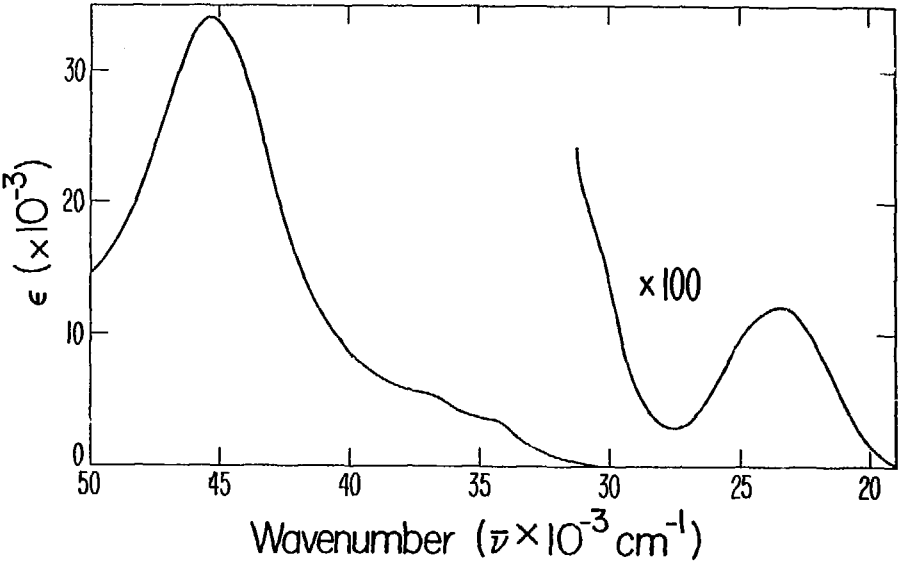
30
20
10
0
ε (x10⁻³)
x100
50
45
40
35
30
25
20
Wavenumber ($\bar{\nu}$ x 10⁻³ cm⁻¹)

XBL 798-2694

Figure 20. Electronic spectrum of $[(Me_5Cp)_2Ni](PF_6)_2$ in 0.10 M aqueous HCl.

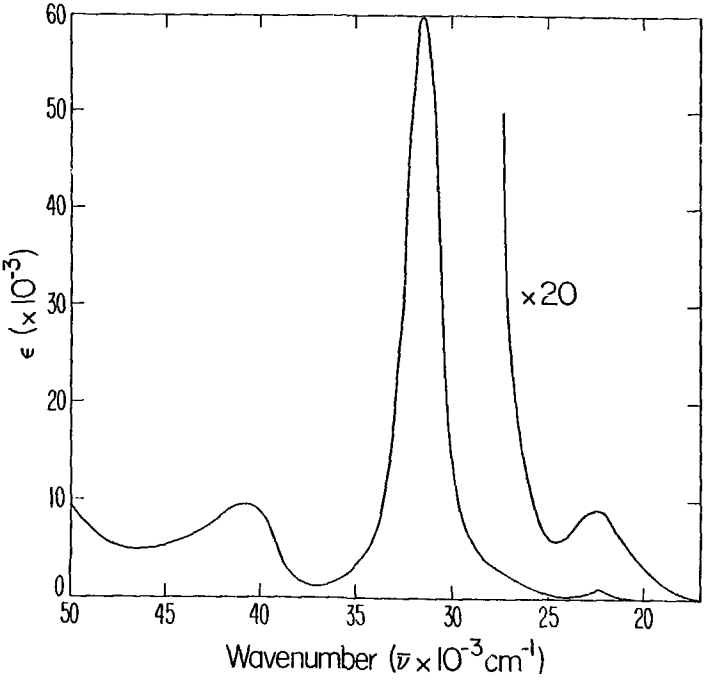
60
50
40
30
20
10
0
ε (x 10^-3)
×20
50
45
40
35
30
25
20
Wavenumber (ν̄ x 10^-3 cm^-1)

XBL 798-2697

transitions. To derive ligand field parameters for the Ni(IV) complex, we have assumed that this transition lies under the 31.5 kK absorption.

The fourth member of the series of $^1A_{1g}$ decamethylmetallocenes, $[(Me_5Cp)_2Mn]^-$, is too air-sensitive to allow an accurate determination of its absorption spectrum. Spectra of $Na[(Me_5Cp)_2Mn]$ in THF solution invariably exhibit peaks attributable to $(Me_5Cp)_2Mn$.

For the 18-electron decamethylmetallocenes, the assignment of the observed ligand field bands follows the pattern established for d^3, d^6, and d^8 Cp_2M compounds.[40,41] The lowest energy singlet absorption band corresponds to the $2a_{1g} \rightarrow 2e_{1g}$ one-electron transition ($^1A_{1g} \rightarrow {}^1E_{1g}(a)$) and the highest energy band is assigned to the $^1A_{1g} \rightarrow {}^1E_{1g}(b)$ transition. The parameters B and Δ_1 are then obtained from appropriate combinations of the transition energy expressions (Table XIII). This calculation confirms the energetic ordering of the excited states, $^1E_{1g}(b) > {}^1E_{2g} > {}^1E_{1g}(a)$, since other assignment schemes yield physically unrealistic (imaginary) values for B. The parameter Δ_2 was calculated with the assumption C = 4B.[35,40] The 12.7, 18.5, and 21.3 kK bands found in the spectrum of $[(Me_5Cp)_2Co]^+$ are assigned to the $^3E_{1g}(a)$, $^3E_{2g}$, and $^3E_{1g}(b)$ excited states, respectively. By a similar analysis, the energy expressions for the spin-forbidden d-d transitions yield B = 680 cm^{-1} and Δ_1 = 13.9 kK, in good agreement with the values determined from the spin-allowed transitions (Table XIII). Calculation of Δ_2 again requires knowledge of the parameter C. A reasonable agreement of the Δ_2 parameters obtained from analysis of the spin-allowed and spin-forbidden transitions is obtained with C = 4.0 (C/B = 5.8-6.3).

Ligand field spectral data and the derived parameters for

Table XIII. Ligand field absorption data and parameters for 18-electron metallocenes and decamethylmetallocenes.[a]

Transition	Cp_2Fe[b]	$(Me_5Cp)_2Fe$	$(Cp_2Co)^+$[b]	$[(Me_5Cp)_2Co]^+$	$[(Me_5Cp)_2Ni]^{2+}$
$^1A_{1g} \rightarrow {}^1E_{1g}(a)$	21.8(36)	23.5(121)	24.3(140)	23.8(330)	22.5(455)
$\rightarrow {}^1E_{2g}$	24.0(72)	30.5(180)	26.4(120)	29.5(1430)	31.5(60,000)[c]
$\rightarrow {}^1E_{1g}(b)$	30.8(49)	34.5(2970)[c]	33.3(1200)	40.0(1170)	42.5(7800)[d]
$\rightarrow {}^3E_{1g}(a)$	18.9(7)	--	21.8(7)	12.7(0.2)	--
$\rightarrow {}^3E_{2g}$	--	--	--	18.5(0.8)	--
$\rightarrow {}^3E_{1g}(b)$	--	--	--	21.3(8)	--
Δ_1	7.1	11.2	7.2	14.1[e]	19.0
Δ_2	22.0	23.1	24.4	24.1[e]	21.5
B	0.39	0.42	0.40	0.63[e]	0.69

a) All energies in kK (10^3 cm^{-1}). Extinction coefficients are enclosed in parentheses. Δ_2 values calculated assuming C/B = 4.0.

b) Data and parameters from reference 40. Ferrocene spectrum measured in 2-methylbutane solution; $(Cp_2Co)ClO_4$ spectrum measured in aqueous solution.

c) Estimated energy of transition.

d) Assignment uncertain.

e) Δ_1, Δ_2 and B values calculated from singlet absorption spectrum. Analysis of spin-forbidden transitions yields B = 0.68 kK and Δ_1 = 13.9 kK.

18-electron metallocenes and decamethylmetallocenes are compared in Table XIII. The Δ_2 parameter is approximately constant in the series of decamethylmetallocenes, but the Δ_1 and B values follow the expected order Ni(IV) > Co(III) > Fe(II). The Δ_2 values determined for $(Me_5Cp)_2Fe$ and $[(Me_5Cp)_2Co]^+$ are comparable to the values found for Cp_2Fe and $[Cp_2Co]^+$, but Δ_1 is 4 to 5 kK greater in the peralkylated systems. The parameter B also increases substantially upon permethylation of the Co(III) complex. The B value for $(Me_5Cp)_2Fe$ is only slightly larger than that found for Cp_2Fe. However, B is very sensitive to the location of the $^1A_{1g} \rightarrow {}^1E_{1g}(b)$ transition. We have assumed a minimum energy for this band in the calculation of B for $(Me_5Cp)_2Fe$, so the true B value may be somewhat larger than that reported.

The peak at 15.9 kK and shoulder at 18.5 kK in the spectrum of $(Me_5Cp)_2Ni$ (Figure 21) are assigned to the $^3E_{1g}(a)$ and $^3E_{2g}$ ligand field excited states, respectively. The third expected d-d band ($^3A_{2g} \rightarrow {}^3E_{1g}(b)$) is apparently submerged under the charge transfer absorptions. Using the intensities of the observed d-d bands as a guide, we find that 25 kK is a reasonable estimate for the minimum energy of the hidden transition: that is, if it occurred below 25 kK it would be resolved at least as a shoulder. With this estimate, the transition energy expressions for $^3A_{2g}$ metallocenes yield B and Δ_1 values comparable to those found for Cp_2Ni, and a Δ_1 value that is 1.5 kK greater in the peralkylated derivative (Scheme I, Table XIV). If the $^3A_{2g} \rightarrow {}^3E_{1g}(b)$ transition is located at a somewhat higher energy (26.5 kK), similar conclusions result. The Δ_2 and B parameters are increased relative to those of Cp_2Ni and Δ_1 is comparable for the two complexes (Scheme II, Table XIV). The

Figure 21. Electronic absorption spectrum of $(Me_5Cp)_2Ni$ in methylcyclohexane solution. Arrow indicates location of shoulder assigned to a ligand field transition.

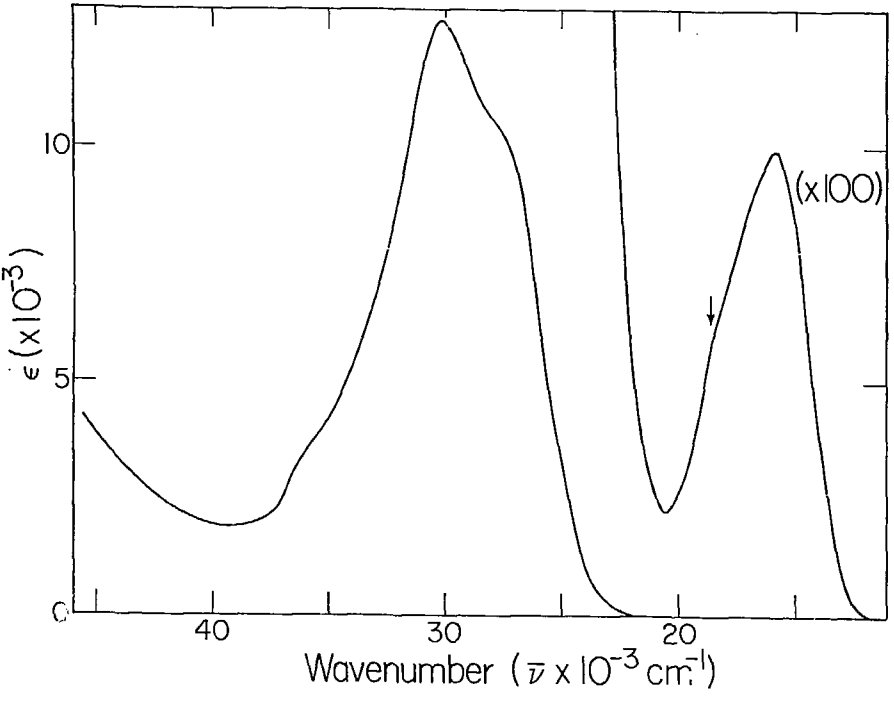

XBL799-2869

Table XLV. Ligand field spectral data and parameters for 20-electron metallocenes and decamethylmetallocenes.[a]

Transition	Cp_2Ni[b]	$(Me_5Cp)_2Ni$	
$^3A_{2g} \rightarrow {}^3E_{1g}(a)$	14.38(62)	15.9(99)	
$\rightarrow {}^3E_{2g}$	16.90(23)	18.5(58)	
$\rightarrow {}^3E_{1g}(b)$	23.45(26)	I 25.0(3250)[c]	II 26.5(3250)[c]
Δ_1	4.60	4.8	4.9
Δ_2	13.92	15.4	15.6
B	0.57	0.58	0.69

a) Energies in kK (10^3 cm^{-1}). Extinction coefficients enclosed in parentheses.

b) Data from reference 109 (measured in n-heptane solution). Parameters from reference 35.

c) Estimated values.

net ligand field splitting ($\Delta_T = \Delta_1 + \Delta_2$) is 1.5 to 2.0 kK greater in $(Me_5Cp)_2Ni$ than in Cp_2Ni.

The absorption spectrum of $(Me_5Cp)_2V$ (Figure 22) exhibits three relatively weak features at 18.7, 20.6, and 28.2 kK that are assigned to the three spin-allowed ligand field transitions, $^4A_{2g} \rightarrow {}^4E_{1g}(a)$, $^4E_{2g}$, $^4E_{1g}(b)$. A ligand field analysis of these bands again shows that the energetic ordering $^4E_{1g}(b) > {}^4E_{2g} > {}^4E_{1g}(a)$ is the only one that gives a non-imaginary B value. The B and Δ_2 values calculated from the transition energy expressions[41] are appreciably larger for $(Me_5Cp)_2V$ than for Cp_2V, but Δ is somewhat smaller in the peralkylated compound (Table XV). The net ligand field splitting ($\Delta_T = \Delta_1 + \Delta_2$) is about 1.1 kK greater for $(Me_5Cp)_2V$ than Cp_2V.

The very weak bands observed in the $(Me_5Cp)_2V$ optical spectrum at 10.5 and 14.5 kK are due to spin-forbidden ligand field transitions. For $^4A_{2g}$ ground state systems, five such transitions are expected to occur in the visible-near infrared region. The orbital occupations, symmetry labels, and transition energy expressions (including configuration interaction between the two $^2E_{2g}$ levels) for these excited states are given below.[63] The

$$^4A_{2g}(e_{2g}^2\ a_{1g}^1) \rightarrow {}^2A_{2g}(e_{2g}^2\ a_{1g}^1) \qquad 3C + 12B$$

$$\rightarrow {}^2A_{1g}(e_{2g}^2\ a_{1g}^1) \qquad 5C + 4B$$

$$\rightarrow {}^2E_{1g}(e_{2g}^2\ a_{1g}^1) \qquad 3C + 4B$$

$$\rightarrow {}^2E_{2g}(a)\ (e_{2g}^3) \qquad 4C + 2B + \Delta_1 - \chi$$

$$\rightarrow {}^2E_{2g}(b)\ (a_{1g}^2\ e_{1g}^1) \qquad 4C + 2B + \Delta_1 + \chi$$

where $\chi = \{(10B - \Delta_1)^2 + (4B+C)^2\}^{1/2}$

Figure 22. Electronic spectrum of $(Me_5Cp)_2V$ in methylcyclohexane solution. Arrows indicate locations of shoulders assigned to spin-allowed ligand field transitions.

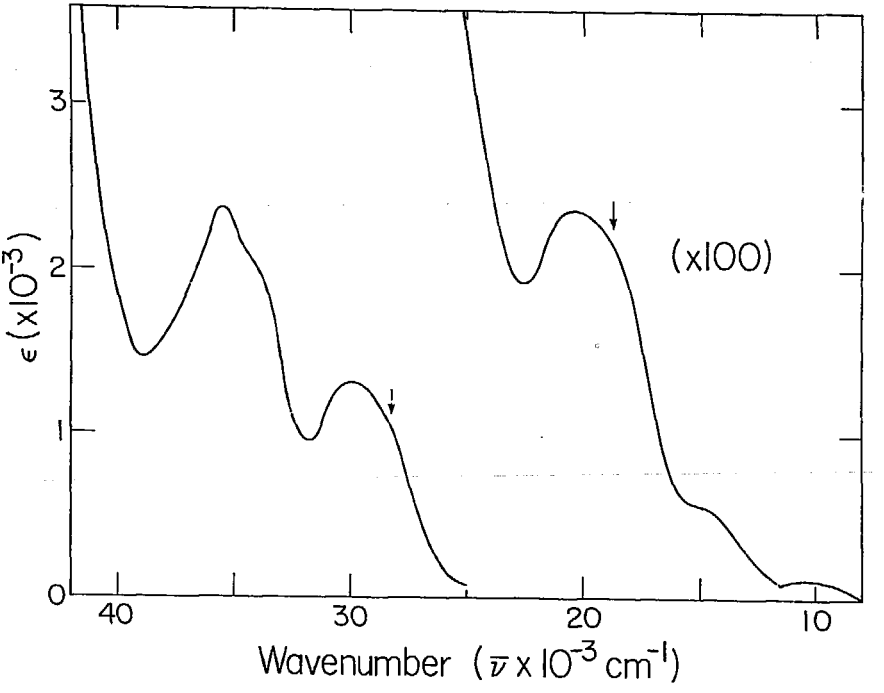

XBL 799-2870

Table XV. Ligand field absorption data and parameters for 15-electron metallocenes and decamethylmetallocenes.[a]

Transition	Cp_2V[b]	$(Me_5Cp)_2V$	$(Cp_2Cr)^+$[c]	$[(Me_5Cp)_2Cr]^+$	
$^4A_{2g} \rightarrow {}^4E_{1g}(a)$	17.33(58)	18.7(23)	17.86(270)	20.4(1386)	
$\rightarrow {}^4E_{2g}$	20.24(46)	20.6(25)	21.98(210)	23.1(2450)	
$\rightarrow {}^4E_{1g}(b)$	24.50(66)	28.2(1037)	27.03(630)	I 29.0(2400)[d]	II 32.0(16,000)[d]
$\rightarrow {}^2E_{1g}$	8.96(.09)	10.5(1.8)	--	--	
$\rightarrow {}^2A_{1g}, {}^2A_{2g}$	13.00(.06)	14.5(5.7)	--	15.4(0.50)	
$\rightarrow {}^2E_{2g}(a)$	--	--	25.0(480)	13.2(0.4)	
$\rightarrow {}^2E_{2g}(b)$	--	--	--	--	
Δ_1	4.93	3.8	6.76	4.9	5.2
Δ_2	16.42	18.7	16.57	19.8	20.2
B	0.42	0.63	0.51	0.54	0.76

a) Energies in kK (10^3 cm^{-1}). Extinction coefficients enclosed in parentheses.

b) Data from reference 110 (measured in diethylether and n-pentane solutions). Parameters from reference 35.

c) Data from reference 87 (measured as I^- salt in aqueous solution). Parameters from reference 35.

d) Estimated value.

14.5 and 10.5 kK absorption bands can be reasonably well accounted for with B = 0.65 and C = 2.5 (C/B = 3.98) if the former is assigned to the $^2A_{1g}$, $^2A_{2g}$ excited states (these are degenerate if C/B = 4) and the latter is assigned to the $^2E_{1g}$ excited state. The $^4A_{2g} \rightarrow {}^2E_{2g}(a)$ transition is predicted to occur at 9.4 kK and this could account for the broadness of the 10.5 kK band.

The shoulders at 20.4 and 23.1 kK in the $[(Me_5Cp)_2Cr]^+$ spectrum (Figure 23) are assigned to the $^4A_{1g} \rightarrow {}^4E_{1g}(a)$, $^4E_{2g}$ transitions. The $^4A_{1g} \rightarrow {}^4E_{1g}(b)$ transition is masked by the charge transfer bands, so we follow the procedure used for $(Me_5Cp)_2Ni$, estimating a minimum (29.0 kK) and maximum (32.0 kK) energy for the absorption to evaluate the ligand field parameters. If the $^4E_{2g}(b)$ excited state lies within this region, the transition energy expressions yield B values ranging from 0.55 to 0.76 (Table XV). While the smaller B value is more consistent with our analysis of the spin-forbidden transitions (vide infra), the larger value results in $B[(Me_5Cp_2)Cr^+] > B[(Me_5Cp)_2V]$, as expected. The ligand field splitting parameters are less sensitive to the location of the $^4E_{2g}(b)$ state. Both estimates give $\Delta_1 \cong 5$ kK (1.7 kK less than for $(Cp_2Cr)^+$) and $\Delta_2 \cong 20$ kK (3.5 kK greater than for $(Cp_2Cr)^+$). The net ligand field splitting is again 1.4 to 2.1 kK larger in the peralkylated complex.

Very weak absorptions are found in the $[(Me_5Cp)_2Cr]^+$ spectrum at 15.4, 13.2, and 8.4 kK. As for $[(Me_5Cp)_2Co]^+$, the 8.4 kK could not be accounted for in terms of a ligand field assignment, so the peak is probably a vibrational overtone. If the 15.4 kK band is assigned to the $^4A_{2g} \rightarrow {}^2A_{2g}, {}^2A_{1g}$ transitions, the $^2E_{2g}(a)$ state

Figure 23. Electronic spectrum of $[(Me_5Cp)_2Cr]PF_6$ in acetonitrile solution. Arrows indicate the location of shoulders assigned to spin-allowed ligand field transitions.

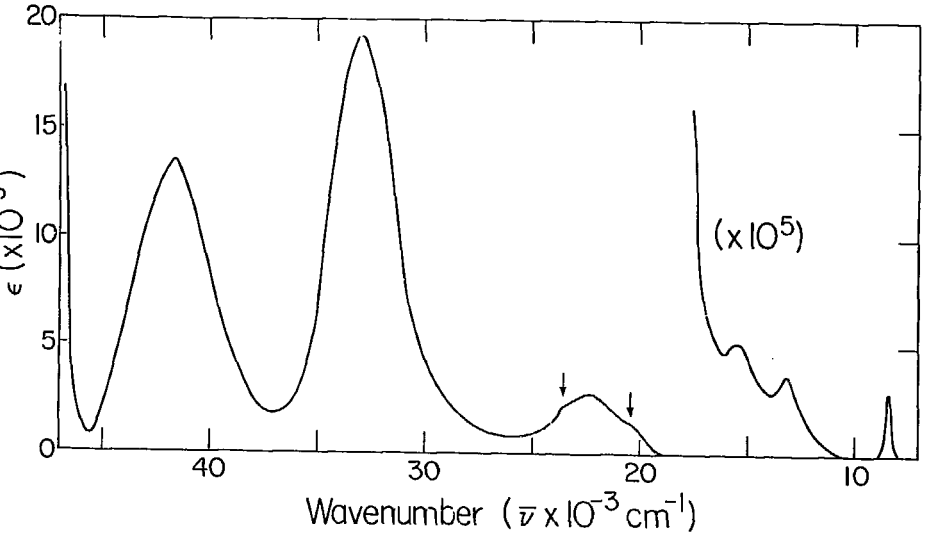

XBL799-2871

is predicted to lie at 12.6 kK, with B = 0.55 and C = 2.9. No other assignments for these two bands yield reasonable values for B and C.

The reader will note that the absorption bands ascribed to spin-forbidden ligand field transitions in the $[(Me_5Cp)_2Cr]^+$ optical spectrum are sharper than those observed in the $(Me_5C_5)_2V$ spectrum. These spin-forbidden transitions should be rather sharp since the ground state and excited state geometries are expected to be similar. For $(Me_5C_5)_2V$, the apparent broadness of the 14.5kK shoulder may be a consequence of its proximity to the much more intense 20.6 kK absorption. As noted earlier, the breadth of the 10.4 kK band may be due to the near coincidence of another spin-forbidden transition, $^4A_{1g} \rightarrow {}^2E_{2g}(a)$.

For the 15-, 18-, and 20-electron systems studied, the ligand field strength of the Cp^- ring is enhanced by complete methylation. For the 18-electron complexes this effect is reflected in a 4000 to 5000 cm^{-1} increase of the ligand field splitting parameter Δ_1 upon permethylation. For the 15- and 20-electron metallocenes, Δ_1 is only modestly affected by peralkylation, but Δ_2 increases by 1500 to 3000 cm^{-1}.

All three spin-allowed d-d transitions are located in the electronic spectra of $[(Me_5Cp)_2Co]^+$ and $(Me_5Cp)_2V$. The B values obtained from a ligand field analysis of the spectra are about 200 cm^{-1} greater than those determined for the unsubstituted compounds. In the case of $(Me_5Cp)_2Fe$, $(Me_5Cp)_2Ni$, and $[(Me_5Cp)_2Cr]^+$, the highest energy ligand field band cannot be located with certainty, but the proposed range of probable energies for the transitions also yields B values that are moderately to significantly increased relative to the unsubstituted compounds. Electrochemical and UV-photoelectron spectral data[63] show that the decamethylmetallocenes

as a class, are more electron-rich than the corresponding metallocenes. We conclude that the increased B values are a result of increased electron density at the metal center in the decamethylmetallocenes.

Summary and Conclusions

The series of $(Me_5Cp)_2M$ compounds (M = Mg,V,Cr,Mn,Fe,Co,Ni) have been prepared and characterized as decamethylmetallocenes. The transition metal derivatives are resistant to hydrolysis and ring exchange reactions, but do undergo facile one-electron oxidation. The $[(Me_5Cp)_2M]^+$ derivatives (M = Cr,Mn,Fe,Co,Ni) are isolable as crystalline PF_6^- salts. These cations are also characterized as D_{5d} or D_{5h} "sandwich" compounds. Oxidation of $(Me_5Cp)_2V$ in donor solvents yields solvated, monocationic derivatives of the form $[(Me_5Cp)_2V(solvent)]PF_6$. A dicarbonyl derivative, $[(Me_5Cp)_2V(CO)_2]PF_6$, can also be prepared, but the pure complex, $[(Me_5Cp)_2V]PF_6$ has not yet proven isolable.

The decamethylmetallocenes and their cationic derivatives are, for the most part, closely related in a chemical and physical sense to their well-known metallocene and metallocene cation counterparts. There are, however, some notable exceptions to this generalization. The decamethylnickelocene dication, $[(Me_5Cp)_2Ni]^{2+}$, can be prepared in aqueous solution and can be isolated as its PF_6^- salt. Nuclear magnetic resonance and UV-visible studies establish that $[(Me_5Cp)_2Ni]^{2+}$ is a diamagnetic, 18-electron complex, isoelectronic with $(Me_5Cp)_2Fe$, $[(Me_5Cp)_2Co]^+$, and $[(Me_5Cp)_2Mn]^-$. Electrochemical studies have indicated that a dicationic derivative of Cp_2Ni has a fleeting existence, but to date there has been no report of either its isolation or characterization in solution.[90,91]

The striking differences in the chemical, physical, and

structural properties of Cp_2Mn and $(Me_5Cp)_2Mn$ were described in Chapter 1. Manganocene[43] is very sensitive to hydrolysis and undergoes rapid ring loss in the presence of $FeCl_2$. It has no well characterized redox chemistry and possesses an abnormally long metal to ring bond. Decamethylmanganocene is rather inert to hydrolysis and ring loss, can be oxidized or reduced to the low-spin 16- and 18-electron derivatives, $[(Me_5Cp)_2Mn]^+$ and $[(Me_5Cp)_2Mn]^-$, and exhibits a metal to ring carbon distance that is comparable to those found for other first transition series decamethylmetallocenes. These differences are related to the observation that $(Me_5Cp)_2Mn$ possesses a low-spin, $^2E_{2g}$, electronic configuration while Cp_2Mn has a high spin, $^6A_{1g}$, ground state. Simple crystal field theory predicts that a low-spin manganocene will possess an enhanced thermodynamic and kinetic stability relative to a high-spin manganocene, as is observed.

In Chapter 1 it was suggested that the low-spin nature of $(Me_5Cp)_2Mn$ is a consequence of the enhancement of the ligand field strength of the $(C_5H_5)^-$ ring by complete replacement of the hydrogens with electron-donating methyl groups. Using a number of physical chemical techniques, the other first transition series metallocenes and decamethylmetallocenes have been compared in order to more quantitatively determine the nature, scope, and magnitude of such an effect.

Magnetic susceptibility and EPR studies of the $(Me_5Cp)_2M$ (M = V,Cr,Co,Ni) and $[(Me_5Cp)_2M]^+$ (M = Cr,Fe,Ni) compounds indicate that they are isoelectronic with their metallocene counterparts. The 16-, 17-, and 19-electron decamethylmetallocenes possess orbitally degenerate ground states. Consequently, the magnetic parameters of these systems are subject to the effects of orbital contributions,

covalency, and distortions from axial symmetry. Calculations utilizing the available EPR data for $(Me_5Cp)_2Mn$ and $[(Me_5Cp)_2Fe]PF_6$ indicate that the covalency (and thus, the bonding character) of the le_{2g} molecular orbital is rather small in the Fe derivative, but much more substantial in the Mn compound. A related calculation based on EPR data for $(Me_5C_5)_2V$ shows the le_{2g} orbital exhibits a significant bonding character in this molecule as well and that the covalency is enhanced by ring peralkylation in this system. These results demonstrate the bonding character of the le_{2g} level is sensitive to changes in the metal ion. This result is not surprising since variations in the sizes and 3d-orbital energies in the first transition series metal ions may be expected to result in changes in the metal-ligand le_{2g} orbital overlap.

Electrochemical studies show that the transition metal decamethylmetallocenes are much more easily oxidized than their corresponding metallocenes. This result reflects the enhanced electron-donor properties of the Me_5Cp^- ligand and indicates that the peralkylmetallocenes are much more electron-rich than the metallocenes.

For d^3, d^6, and d^8 systems, the ligand field absorption bands occur at higher energy in the $(Me_5Cp)_2M$ compounds than in the Cp_2M derivatives. A ligand field analysis of the spectra shows that the net ligand field splitting is larger in the peralkylated complexes than in the unsubstituted compounds. The effect is quite substantial in the d^6 Fe(II) and Co(III) systems where Δ_1 increases by 4000 to 5000 cm^{-1} upon peralkylation. The electron repulsion parameter, B, is greater in the peralkylated metallocenes as well. This is another indication that the metal centers are more electron-rich in the decamethylmetallocenes than in the corresponding metallocenes.

References

1. Kealy, T. J.; Pauson, P. L. Nature 1951, 168, 1039-1040.
2. Wilkinson, G.; Rosenblum, M.; Whiting, M.C.; Woodward, R. B. J. Am. Chem. Soc. 1952, 74, 2125-2126.
3. Fischer, E. O.; Pfab, W. Z. Naturforschg. 1952, 74, 2125-2126.
4. Coates, G. E.; Green, M. L. H.; Wade, K. "Organometallic Compounds", 3rd edition; Methuen: London, 1967.
5. Marks, T. J. Prog. Inorg. Chem. 1978, 24, 51-107.
6. Marks, T. J. Prog. Inorg. Chem. 1979, 25, 223-333.
7. Threlkel, R. S.; Bercaw, J. E. J. Organomet. Chem. 1977, 136, 1-5.
8. Feitler, D.; Whitesides, G. M. Inorg. Chem. 1976, 15, 466-469.
9. Schmitt, G.; Özman, S. Chem. Zeit., 1976, 100, 143.
10. Bercaw, J. E.; Marvich, R. H.; Bell, L. G.; Brintzinger, H. H. J. Am. Chem. Soc. 1972, 94, 1219-1238.
11. Bercaw, J.E. J. Am. Chem. Soc. 1974, 96, 5087-5095.
12. Manriquez, J. M.; McAlister, D.R.; Sanner, R.D.; Bercaw, J. E. J. Am. Chem. Soc. 1978, 100, 2716-2724.
13. King, R. B. Coord. Chem. Rev. 1976, 20, 155-169, and references therein.
14. Rigby, W.; McCleverty, J.A.; Maitliss, P. M. J. Chem. Soc., Dalton Trans. 1979, 382-386, and references therein.
15. Green, M. L. H.; Pardy, R. B. A. J. Chem. Soc., Dalton Trans., 1979, 355-360.
16. McLain, S. J.; Wood, C. D.; Schrock, R. R. J. Am. Chem. Soc. 1979, 101, 4558-4570.

17. Green, J.C.; Watts, O. J. Organomet. Chem. 1978, 153, C40.

18. Manriquez, J. M.; Fagan, P. J.; Marks, T. J. J. Am. Chem. Soc. 1978, 100, 3939-3941.

19. Manriquez, J. M.; Fagan, P. J.; Marks, T. J.; Vollmer, S. H.; Day, C. S.; Day, V. W. J. Am. Chem. Soc. 1979, 101, 5075-5078.

20. Webb, I. B.; Collins, D. M.; Cotton, F. A.; Baldwin, J. C.; Kaska, W. C. J. Organometal. Chem. 1979, 165, 373-381.

21. Mise, T.; Yamazaki, H. J. Organomet. Chem. 1979, 164, 391-400.

22. Cooper, N. J.; Green, M. L. H.; Couldwell, C.; Prout, K. J. Chem. Soc. Chem. Comm. 1977, 145-146.

23. Smart, J. C.; Curtis, C. J. Inorg. Chem. 1978, 17, 3290-3292.

24. Davison, A.; Wreford, S. S. J. Am. Chem. Soc. 1974, 96, 3017-3018.

25. Tebbe, F. N.; Parshall, G. W. J. Am. Chem. Soc. 1971, 93, 3793-3795.

26. Guggenberger, L. J.; Tebbe, F. N. J. Am. Chem. Soc. 1971, 93, 5924-5925.

27. Fischer, E. O.; Hristidu, Y. Z. Naturforschg. 1962, 17b, 275.

28. Fischer, E. O.; Treiber, A. Z. Naturforschg. 1962, 17b, 276.

29. Ter Haar, G. L.; Dubek, M. Inorg. Chem. 1964, 3, 1648-1651.

30. Wilkinson, G.; Reynolds, L. T. J. Inorg. Nucl. Chem. 1956, 2, 246-253.

31. Doretti, L.; Zanella, P.; Faraglia, G.; Faleschini, S. J. Organomet. Chem. 1972, 43, 339-341.

32. Ernst, R. D.; Kennelly, W. J.; Day, C. S.; Day, V. W.; Marks, T. J. J. Am. Chem. Soc. 1979, 101, 2656-2664.

33. Bagnall, K. W., "Inorganices of the f-Elements", Marks, T.J.; Fischer, R. D., eds. D. Reidel: Dordrecht, 1979, 221-248.

34. King, R. B. Organometallic Syntheses, 1965, 1, 63-72, and references therein.

35. Warren, K. D. Struct. Bonding 1976, 27, 45-159, and references therein.

36. Rettig, M. F. "NMR of Paramagnetic Molecules: Principles and Applications", LaMar, G. N.; Horrocks, W.; Holm, R. H., eds. Academic Press: New York, 1973, 218-241, and references therein.

37. Ballhausen, C. J.; Gray, H. B. "Coordination Chemistry" vol. 1, Martell, A. E., ed. Van Nostrand Reinhold: New York, 1971, 3-83.

38. a) Zerner, M. C.; Loew, G. H.; Kirchner, R. F.; Mueller-Westerhoff, U. T. J. Am. Chem. Soc. 1980, 102, 589-599.

b) Coutierê, M. M.; Demuyuck, J.; Veillard, A. Theor. Chim. Acta. 1978, 27, 281-287.

c) Rosch, N.; Johnson, K. Chem. Phys. Lett. 1974, 24, 179-184.

d) Bagus, P. S.; Wahlgren, U. I.; Alflof, J. J. Chem. Phys. 1976, 64, 2324-2334.

e) Ammeter, J. H.; Burgi, H. B.; Thibault, J. C.; Hoffman, R. J. Am. Chem. Soc. 1978, 100, 3686-3692.

39. a) Wertheim, G.; Herbes, R. H. J. Chem. Phys. 1963, 38, 2106-2109 and references therein.

b) Walker, L. R.; Wertheim, G. K.; Jaccarino, V. Phys. Rev. Lett. 1961, 6, 98-102.

c) Prins, R.; Kortbeck, A. J. Organometal. Chem. 1971, 33, C33-35.

40. Sohn, Y. S.; Hendrickson, D. N.; Gray, H. B. J. Am. Chem. Soc. 1971, 93, 3603-3612.

41. Prins, R.; van Voorst, J. D. W. J. Chem. Phys. 1968, 49, 4665-4673.

42. a) Evans, S.; Green, M. L. H.; Jewitt, B.; Orchard, A. F.; Pygall, C. F. J. Chem. Soc. Faraday Trans. 2 1972, 68, 1847-1865.

b) Evans, S.; Green, M. L. H.; Jewitt, B.; King, G. H.; Orchard, A. F. J. Chem. Soc. Faraday Trans. 2 1974, 70, 356-376.

43. Wilkinson, G.; Cotton, F. A.; Birmingham, J. M. J. Inorg. Nucl. Chem. 1956, 2, 95-113.

44. Bunder, W.; Weiss, E. Z. Naturforschg. 1978, 33b, 1235-1237.

45. King, R. B.; Bisnette, M. B. J. Organomet. Chem. 1967, 8, 287-297.

46. a) Jolly, W. L. "The Synthesis and Characterization of Inorganic Compounds", Prentice-Hall: Englewood Cliffs, N.J., 1970.

b) Pinsky, B. L., Dissertation, University of California, Berkeley, 1979.

47. Most of the results described in Chapter 1 have been published:

a) Smart, J. C.; Robbins, J. L. J. Am. Chem. Soc. 1978, 100, 3936-3937.

b) Robbins, J. L.; Edelstein, N. M.; Cooper, S. R.; Smart, J. C. J. Am. Chem. Soc. 1979, 101, 3853-3857.

c) Freyberg, D. P.; Robbins, J. L.; Raymond, K. N.; Smart, J. C. J. Am. Chem. Soc. 1979, 101, 892-897.

d) Fernholt, L.; Haaland, A.; Seip, R.; Robbins, J. L.; Smart,

J. C. J. Organometal. Chem. 1980, 194, 351-357.

48. Duggan, D. M.; Hendrickson, D. N. Inorg. Chem. 1975, 14, 955-970.

49. Reynolds, L. T.; Wilkinson, G. W. J. Inorg. Nucl. Chem. 1954, 9, 86-92.

50. Orgel, L. E. "An Introduction to Transition Metal Chemistry", 2nd ed.; Wiley: New York, 1960; pp. 78-79.

51. Almenningen, A.; Samdal, S.; Haaland, A. J. Chem. Soc. Chem. Commun. 1977, 14-15.

52. Basolo, F.; Pearson, R. G. "Mechanisms of Inorganic Reactions", 2nd ed.; Wiley: New York, 1967, pp. 145-148.

53. Taube, H. Chem. Rev. 1952, 50, 69-110.

54. Cooke, A. H.; Duffus, H. J. Proc. Phys. Soc., London, Sect. A 1955, 68, 32-38.

55. Goldenberg, N. Trans. Faraday Soc. 1940, 36, 847-856.

56. Nicholson, R. S.; Shain, I. Anal. Chem. 1964, 36, 706-723.

57. Similar reactions with Cp_2Mn or $(MeCp)_2Mn$ did not yield tractable products.

58. a) Geiger, W. E., Jr., J. Am. Chem. Soc. 1974, 96, 2632-2634. b) Holloway, J. D. L.; Bowden, W. L.; Geiger, W. E., Jr. J. Am. Chem. Soc. 1977, 99, 7089-7090.

59. Evans, D. F. J. Chem. Soc. 1959, 2003-2005.

60. Freyberg, D. P.; Robbins, J. L.; Hollander, F.; Raymond, K. N.; Smart, J. C., unpublished results.

61. Reynolds, L. T.; Wilkinson, G. J. Inorg. Nucl. Chem. 1959, 9, 86-92.

62. Switzer, M. E.; Wang, R.; Rettig, M. F.; Maki, A. H. J. Am.

Chem. Soc. 1974, 96, 7669-7674.

63. Cauletti, C.; Green, J. C.; Kelly, M. R.; Powell, P.; van Tilborg, J.; Robbins, J.; Smart, J. J. Elect. Spec., 1980, 19, 327-357.

64. Ammeter, J. H.; Bucher, R.; Oswald, N. J. Am. Chem. Soc. 1974, 96, 7833-7835.

65. Warren, K. D. Inorg. Chem. 1974, 13, 1317-1324.

66. Gordon, K. R.; Warren, K. D. Inorg. Chem. 1978, 17, 987-994.

67. The UV-PES studies of $(MeCp)_2$ indicate that it exists in equilibrium between high-spin ($^6A_{1g}$) and low-spin ($^2E_{2g}$) electronic configurations in the gas-phase. See references 42b, 63.

68. Ammeter, J. H. J. Magn. Reson. 1978, 30, 299-325.

69. Maki, A. H.; Berry, T. E. J. Am. Chem. Soc. 1965, 87, 4437-4441.

70. Almenningen, A.; Haaland, A.; Motzfeldt, T. "Selected Topics in Structure Chemistry", Universitetsforlaget: Oslo, 1967; p. 105.

71. Haaland, A.; Lusztyk, J.; Novak, D. P.; Brunvoll, J.; Sarovieysky, K. B. J. Chem. Soc. Chem. Commun. 1974, 54-55.

72. a) Almenningen, A.; Haaland, A.; Samdal, S. J. Organomet. Chem. 1978, 149, 219-229.

b) Haaland, A. Acc. Chem. Res. 1979, 12, 415-422.

73. Almenningen, A.; Gard, E.; Haaland, A.; Brunvoll, J. J. Organomet. Chem. 1976, 107, 273-279.

74. Haaland, A.; Nilsson, J. E.; Acta Chem. Scand. 1968, 22, 2653-2670.

75. Hedberg, A. K.; Hedberg, L.; Hedberg, K. J. Chem. Phys. 1975, 63, 1262-1266.

76. Hedberg, L.; Hedberg, K.; J. Chem. Phys. 1970, 53, 1228-1234.

77. Gard, E.; Haaland, A.; Novak, D. P.; Seip, R. J. Organomet. Chem.

1975, 88, 181-189.

78. Almenningen, A.; Haaland, A.; Samdal, S.; Brunvoll, J.; Robbins, J. L.; Smart, J. C. J. Organomet. Chem. 1979, 173, 293-299.

79. Kohler, F. H.; Prossdorf, W. Z. Naturforschg. 1977, 32b, 1026-1029.

80. Jutzi, P.; Kohl, F. J. Organomet. Chem. 1979, 164, 141-152.

81. Khamar, M. M.; Larkworthy, L. F.; Patel, K. C.; Phillips, D. J.; Beech, G. Aust. J. Chem. 1974, 27, 41-51.

82. Rettig, M. F.; Drago, R. S. J. Am. Chem. Soc. 1969, 91, 1361-1370.

83. Green and Pardy (reference 15) recently found that (ethyltetramethylcyclopentadienyl)tin tri-n-butyl reacts with $CoCl_2$ in THF solution to yield a toluene-soluble, red-brown oil. Chlorination of this oil afforded complexes of the stoichiometry, $[(EtMe_4Cp)CoCl_2]_2$ and $[(EtMe_4Cp)_2Co_3Cl_6]$ ($EtMe_4Cp$ = η-ethyltetramethylcyclopentadienyl). These compounds dissolved in water to give blue solutions of the trichloro-bridged dimer, $[(EtMe_4Cp)_2Co_2(\mu\text{-}Cl_3)]^+$. The structure of this cation (as the $FeCl_4^-$ salt) has been determined by X-ray crystallography (see reference 84). No mononuclear metallocene or metallicenium products were isolated.

84. Couldwell, C.; Husain, J. Acta Cryst. 1978, B34, 2444-2450.

85. Koelle, U.; Khouzami, F. Angew. Chem. Int. Ed. 1980, 19, 640-641.

86. $(Me_5Cp)_2Mg$ decomposes in acetone or acetonitrile.

87. Fischer, E. O.; Ulm, K. Chem. Ber. 1962, 95, 692-694.

88. Fischer, E. O.; Ulm, K.; Kuzel, P. Z. Anorg. Allgem. Chem. 1963,

319, 253-265.

89. Pinsky, B. L. personal communication.

90. Wilson, R. J.; Warren, L. F.; Hawthorne, M. F. J. Am. Chem. Soc. 1969, 91, 758-759.

91. Van Duyne, R. P.; Reilley, C. N. Anal. Chem. 1972, 44, 158-169.

92. De Liefde Meijer, H. J.; Janssen, M. J.; Van Der Kerk, G. J. M. Rec. Trav. Chim. Pays-Bas 1961, 80, 831-845.

93. Fachinetti, G.; Del Nero, S.; Floriani, C. J. Chem. Soc. Dalton Trans. 1976, 1046-1049.

94. Calderazzo, F.; Fachinetti, G.; Floriani, C. J. Am. Chem. Soc. 1974, 96, 3695-3696.

95. Calderazzo, F.; Bacciarelli, S. Inorg. Chem. 1963, 2, 721-723.

96. Leipfinger, H. Z. Naturforschg. 1958, 13b, 53-54.

97. Englemann, F. Z. Naturforschg. 1953, 8b, 775-776.

98. Fritz, H. P.; Schwarzhans, K. E. J. Organomet. Chem. 1964, 1, 208-211.

99. Fischer, E. O.; Jira, R. Z. Naturforschg. 1953, 8b, 217-219.

100. Prins, R.; Van Voorst, J. D. W.; Schinkel, C. J. Chem. Phys. Lett. 1967, 1, 54-55.

101. Nussbaum, M.; Voitländer, J. Z. Naturforschg. 1965, 20a, 1411-1416.

102. Nussbaum, M.; Voitländer, J. Z. Naturforschg. 1965, 20a, 1417-1424.

103. McConnel, H. M.; Porterfield, W. W.; Robertson, R. E. J. Chem. Phys. 1959, 30, 442-443.

104. Ammeter suggests that the A_{4s} term of equation 2 (reference 41) should be divided by three to account for the presence of only

one of the three unpaired electrons in the a_{1g} level. See p. 116 of reference 55.

105. Ammeter, J. H.; Oswald, N.; Bucher, R. Helv. Chim. Acta 1975, 58, 671-682.

106. Ammeter, J. H.; Swalen, J. D. J. Chem. Phys. 1972, 57, 678-698.

107. Ammeter, J. H.; Brom, J. M. Jr. Chem. Phys. Lett. 1974, 27, 380-384.

108. Bucher, R. Dissertation. Eidgenössischen Technische Hochschule, Zurich, 1977.

109. Pavlik, I.; Cerny, V.; Maxova, E. Coll. Czech. Chem. Commun. 1970, 35, 3045-3063.

110. Pavlik, I.; Cerny, V.; Maxova, E. Coll. Czech. Chem. Commun. 1972, 37, 171-195.

111. Single crystal EPR and UV-visible studies of the decamethylmetallocenes are being carried out in the laboratory of Professor Dr. John Ammeter at the University of Zurich.